JIMMA UNIVERSITY

JIMMA INSTITUTE OF TECHNOLOGY

SCHOOL OF GRAUATE STUDIES

DEPARTMENT OF CIVIL ENGINEERING

RESPONSE ANALYSIS OF RC SHEAR WALL USING FINITE ELEMENT METHOD SUBJECT TO BLAST LOADS

BY

Haymanot G/Sillasie

A thesis submitted To School of Graduate Studies of Jimma Institute of Technology, In Partial Fulfillment of Requirements for Degree of Masters Of Science in Structural Engineering

Nov, 2016

Jimma, Ethiopia

JIMMA UNIVERSITY

JIMMA INSTITUTE OF TECHNOLOGY

SCHOOL OF GRAUATE STUDIES

DEPARTMENT OF CIVIL ENGINEERING

RESPONSE ANALYSIS OF RC SHEAR WALL USING FINITE ELEMENT METHOD SUBJECT TO BLAST LOADS

BY

Haymanot G/Sillasie

A thesis submitted To School of Graduate Studies of Jimma Institute of Technology, In Partial Fulfillment of Requirements for Degree of Masters of Science In Structural Engineering

Main Adviser: Dr Temesgen Wondimu

Co_ Adviser: Eng. Bobby Lupango

Nov, 2016

Jimma, Ethiopia

Response Analysis of RC Shear Wall using Finite Element Method Subject to Blast Loads

Declaration

I certify that this research entitled "Response Analysis of RC Shear Wall Using Finite Element Method Subject to Blast Loads" is my original work. This work has not been presented for a degree or for diploma in any other university.

Name: Haymanot G/Silassie

Signature__________ Date 15/11/2016

Place: Jimma

Adviser

Main adviser: Dr Temesgen Wondimu

Signature__________ Date 15/11/2016

Co adviser: Eng. Bobby Lupango

Signature__________ Date 15/11/2016

SCHOOL OF POST GRADUATE STUDIES

JIMMA UNIVERSITY

As members of the examining board of the final MSc open defense, we certify that we have read and evaluated the thesis prepared by Haymanot G/Silassie entitled: "**Response Analysis OF RC Shear Wall Using Finite Element Method Subject To Blast Loads**"and recommended that it would be accepted as fulfilling the thesis requirement for the degree of Master of Science in Structural Engineering.

Dr.Ing. Temesgen Wondimu (PhD) Advisor	Signature	2nd dec 2016 Date
Eng.Bobby Lupango (MSc) Co-advisor	Signature	2nd dec 2016 Date
Dr. Ing. Abrham Gebre (PhD) External examiner	Signature	NOV.30, 2016 Date
Eng. Vinod Kumar (MSc) Internal examiner	Signature	2nd dec 2016 Date
Eng.V.S. Ravi Kumar(MSc) Chairman	Signature	2nd Dec 2016 Date

Acknowledgements

First I want to thank my lord for all things happened in my life. Second I would like to thank my advisor Dr Temesgen Wondimu for giving me the time, courage, patience and continuous supervision for determination of doing this thesis.

I also would like to thank my co-advisor Eng. Bobby Lupango for his continuous support.

I am also would like to thank Ethiopian roads authority and Jimma University together for giving me a full scholar ship for Msc program.

Last but not least thank you to my all nearest friends and my dearest families for their encouragement throughout my master's program and support throughout the process of this research.

Table of contents

LIST OF TABLES

LIST OF FIGURES

Figures **Page**

Acronyms

RC	Reinforced Concrete
FEM	Finite Element Method
JIT	Jimma Institute of Technology
EBC	Ethiopian Building Code
EC	European Code
CDP	Concrete Damage Plasticity
Pso	Peak pressure

List of Notations

Φ	Diameter of the reinforcement bar
R	Distance of bomb from target
Z	Scale distance
ϵcpl	plastic compression strain
ϵtp	plastic tensile strain
E_S	Young's modulus of elasticity of steel
E_C	Young's modulus of elasticity of concrete
ω_{max}	The maximum frequency
Le	The length of the element
Cd	The propagation velocity of dilatational waves
Δt	Increment time
ρ	Reinforcements ratio
S	Center to center distance (spacing) between reinforcement bars
fc*	Yield stress of concrete material
δ_2	Displacement in the Y-direction
δ_3	Displacement in Z- direction
f_{22}	Stress on Y direction

Abstract

Shear walls are used as one of the primary lateral load resisting components in lightweight framing of low and mid-rise residential constructions. In this thesis, the behavior of reinforced concrete shear wall under blast will be investigated by using finite element method. The finite element model considers geometric nonlinearities caused by large deformation as well as materials nonlinearities. In addition to nonlinearities, study is also carried out to investigate the effect of standoff distance from RC shear wall location to bomb location, radial direction of loading and type of shear wall.

In this study, blast load response of RC shear wall with the same mesh size, different standoff distances, and different radial direction of loading and different cross sectional shape was investigated.

Finite element model of RC shear wall are developed in ABAQUS 6.13 and the blast loads taken as pressure loads, close in case at1m standoff distance, near field at 3m and 7m standoff distances and also far field cases at 11m standoff distance from the location of RC shear wall.

The response of RC shear wall to blast loading studied by using displacement time history curve and von mise stress time history curve for each standoff distances, for the three radial location of loads and for each type of RC shear walls, from this study, it is observed that an increasing the standoff distance from 1m to 11m, decrease the corresponding deflection and stress of the RC shear wall structure. Another result observed from this study is the bomb load placed at rear side of Inverted RC shear wall, the deflection decrease from the three radial directional location of blast. This study concludes, from the three types of RC shear walls, Inverted RC shear wall type is the more effective on resistance of bomb load.

Keywords: Finite Element method, Reinforced Concrete Shear wall, Blast Loads

CHAPTER ONE

INTRODUCTION

1.1 Background

RC is a composite material consisting of concrete and reinforcing steels. Walls are one of the structures used to resist lateral loads. There are different types of walls, such as bearing walls, non-bearing walls, shear walls, flexural shear walls, and structural type squat shear walls. From these walls, shear walls are part of the lateral force resisting systems that carry loads, bending moments about the wall strong axis, and shear forces parallel to the wall length. Shear wall system is one of the most common and effective lateral load resisting systems that are widely used in buildings. It can provide the adequate strength and stiffness needed for the building to resist lateral loads like earthquake load, wind loads and blast loads.

Blast loads are high energy dissipation loads. The blast load may occur in different ways but for this research, the blast load type is bomb. This blast load occurs in different magnitude.

During the recent years, an enormous effort has been done to provide analytical models that are able to simulate the actual behavior of RC shear walls. The wide uses of computers help to develop more sophisticated models that can have different load phenomena. For these models to be verified, experimental research is continuously conducted on RC shear walls tested under monotonic, cyclic, or dynamic loading. The numerical modeling of RC walls is not involved only in the applications for new construction, but it is also extended to the applications of existing structures. Response of an existing RC shear wall under certain lateral load hazard, and to predict its expected mode of failure in order to be able to choose the most suitable and effective retrofitting technique for wall that would meet a target performance.

Various numerical methods have been developed for the analysis of reinforced concrete and concrete structures. In order to investigate the issues such as modeling techniques and stiffness of nonstructural components, extensive computational studies are being conducted before and after the test. Among several types of analysis, the post-test analysis results by the finite element model using shell elements is reported to investigate the effects of stiffness on the collapse behavior

Blast loads are one of the types of loads which have an effect on dynamic behaviors of the reinforced concrete structures. Different approaches are available to estimate the response of RC shear walls subject to blast loads: experimental, analytical and numerical methodologies. In order to overcome the limitations of the experimental approach, Finite element methods can be used to evaluate the response of RC shear walls under blast loads condition. Therefore for this thesis, the numerical method of finite element method is preferable

In recent years, because of increased fanatic activities, civil structures are exposed to threats from blast-induced impulsive loads. Several such incidents have taken place around the world, causing serious threat to life and property. Furthermore, extremists are using newer chemicals and technological advancements that have increased blast event magnitudes. Therefore, in addition to protect strategically important and heritage structures, even important commercial buildings and complexes are required to be designed for an adequate level of blast resistance.

.The aim of this thesis is to study the modeling ,response and behavior of reinforced concrete shear walls subjected to blast loads.

1.2. Statement of the Problem

There are different types of loads applied on structure. From this type of loads lateral load is one of the load types which occur due to seismic condition and another type of loads from explosive called blast loads. Blast loads has need a careful attention, because it affect the life of creatures and damage properties of peoples. Generally, Blast loads (bomb) have an effect on the performance of reinforced concrete structure like shear wall. But, in our country provisions and special consideration to predict the effect of blast loads lack in current Ethiopian practice in design of every type of structural components specially RC shear wall. Therefore, response of RC shear wall on blast load using finite element method is the main focus of this study.

So far, from previous related studies, there were different mechanisms by which analysis of reinforced concrete structures but more attention is giving for finite element method.

Therefore, the research study proposes to conduct analysis of reinforced concrete shear wall subjected to blast loads using finite element method. To achieve the objectives of the research study a review of related literatures, organization of input data and finite element method for analysis will be undertaken.

1.3. Methodology

The simulations performed using ABAQUS 6.13.This software is used since it has numerous material models in its material library and provides various types of element formulation in its library. Perfect bond between steel bars and concrete has been modeled by defining bonded interface between them using constraint command of ABAQUS 6.13. A solid element is used for concrete and a beam element (truss) is used for horizontal and vertical reinforcement bars.

In order to employ proper finite element models to analyze and study the performance of the shear walls subjected to blast loads like bomb, shear wall is modeled considering geometric as well as materials nonlinearities.

1.4 Objective of the study

Blast affects the nonlinear response of reinforced concrete shear wall. For analysis of blast loads on structure, radial directions and standoff distances are the basic factors which affect the RC shear wall. In this research, the effect of standoff distance, radial direction of bomb location with different cross section of RC shear wall investigated.

This study generally has the following objectives

1.4.1. General objectives

To investigate the response of reinforced concrete shear wall to blast loads.

1.4.2. Specific Objectives

To determine the effect of standoff distances to the magnitude of blast or bomb loading

To determine the effect of radial direction of bomb loads locations.

To select from the rectangular cantilever section, Inverted u- section and from T-section RC shear wall for the most effective section in resisting blast load.

1.5. Scope of the study

In order to accomplish the above listed objectives, the following works performed.

Generate the finite element model for the given cross-sectional shape of RC shear wall with two directional reinforcements and Inverted u-section RC shear wall and T-section RC shear wall. Apply fixed boundary conditions at bottom of RC shear walls. Subject the shear wall with different standoff distance and different radial direction of bomb and study relation of each material property with standoff distance.

Subject the RC shear wall to bomb with different standoff distance and same weight of bomb and generate the response of RC shear wall.

Compare the result with the result of types of shear wall and study the response of the structure.

1.6. Thesis organization

This research is organized into the following six chapters

Chapter 1: Explanation about blast load and Finite element method

Chapter 2: Discussion of different related literature on blast loads.

Chapter 3: Discusses the methodology to model the RC hear walls and investigate the effect of RC shear walls and the materials used in modeling of structure using finite modeling analysis

Chapter 4: Show the validation of the blast loads response

Chapter 5: Results and discussions of blast loads response

Chapter 6: Discusses the conclusion from the above chapters and indicate the recommendation for future works.

CHAPTER TWO

LITERATURE REVIEW

2.1 Introduction

Now a day most buildings are constructed by reinforced concrete materials. Shear wall is one of the structural components of any structure which can construct from RC materials. Every Re searcher addressed research related to blast loads. Numerous data that studies have been undertaken to analyze the structure by using practical test in laboratory and software for modeling and analysis. Here all studies describes in this chapter, gives an idea about the previous studies of various researchers done in the modeling and analysis of structures related to blast loads. Generally the characteristics or behavior of the structure under blast loads have also been discussed.

2.2. Blast Load

Loads are usually divided into static loads, quasi static loads and dynamic loads based on the time duration of an action. There are different event and researches which had been done on blast loads analysis of structures especially bombs. Research done on nonlinear analysis of reinforced concrete slabs subjected to blast loading shows, the time duration is an important parameters since it has an influence on the response of reinforced concrete slabs. The second important parameter that has to be considered when designing reinforced concrete structure against blast loading is dimension of the structure. Additional critical parameters like the stand- off distance and the equivalent weight of bomb (explosive) materials must be also accounted when analyzing reinforced concrete structure [1].

The threat for a conventional bomb is defined by two elements, bomb size (charge weight W) and stand of distance (R) between blast source and the target. The pressure is related to a factor called scale distance (Z).As the distance increases, the maximum pressure of the shock wave decrease. They should also be noted that at any particular range, the peak overpressure of the blast wave decays exponentially to the atmospheric pressure [2]. The scaled distance is given by

$$Z = \frac{R}{\sqrt[3]{W}} \tag{2.1}$$

Where: R=Distance from blast source

W= mass of charge in terms of TNT

There are different methods to estimate blast loads and structural response,blast wave parameters for conventional high explosive materials have been the focus of a number of studies during the 1950’s and 1960’s.Estimations of peak overpressure due to spherical blast based on scale distance were introduced [3]. The over pressure are given by

$$p_{so} = \frac{6.7}{z^{3}} + 1bar\,(p_{so} > 10bar) \tag{2.2a}$$

$$p_{so} = \frac{0.975}{z} - \frac{1.455}{z^{2}} + \frac{5.85}{z^{3}} - 0.019bar \tag{2.2b}$$

$$0.1bar < p_{so} < 10bar$$

In simmilar manner Nemark and Hansen introduced a calculation of maximum blast overpressure, p_{so} in bars,for a high explosive charge that detonates at the ground surface as:

$$P_{SO} = 6784\frac{W}{R^{2}} + 93\sqrt{\frac{W}{R^{3}}} \tag{2.2c}$$

Another expression of peak over pressure in kPa is introduced by Mills,in which is expressed as the equivalent charge weight in Kg of TNT, and Z is the scaled distance.

$$p_{so} = 1772\frac{1}{z^{3}} + 114\frac{1}{z^{2}} + 108\frac{1}{z} \tag{2.2d}$$

The first application of the finite element method of analysis of analysis of RC elements was started by nonlinear macro model.since several advancements were done in the area of modeling of RC elements including shear walls [4].

Researchers argue that using a numerical, finite element method for modeling and analysis of structure under blast loads analysis is one of the methods for analysis of structure. Before analysis of structure, the first step is modeling of the structure. Modeling of reinforced concrete shear wall subject to blast loads, have reinforcing steel and concrete materials to model the shear wall. Research done on similar subject of reinforced concrete structure concluded that simplifying assumptions for the structure and materials are allowable for this kind of analysis and that this is the only way of successfully run a complete analysis of an entire building [5].

Research done on blast describes the process of determining the blast load on structures and provides a numerical example of a structure exposed to this load. The blast load was analytically determined by pressure-time history and a numerical model of the structure was created by SAP2000. The results confirm the initial assumption that it is possible with conventional software to simulate an explosion effects and give a preliminary assessment of structure. Therefore the researcher conclude that for the element exposed to distant explosion ,conventional reinforcement provides sufficient ductility, while for close explosions additional reinforcement is needed [6].

2.3 Finite Element Modeling

ABAQUS User Manual, describes the non- linear finite element software package ABAQUS that is employed for analysis. In this study all beams are modeled. Steel bars are embedded in concrete creating a perfect bond between concrete and steel. The advantage of the embedded model is that it allows independent mesh of elements [7].

Non-linear analysis of reinforced concrete structure under blast loads can be done by using finite element analysis software. There are lots of researches that done with finite element analysis software. The research done on modeling of reinforced concrete columns which is subject to axial loads and lateral blast loads shown, using finite element package ABAQUS is the preferable analysis software with design considerations for adverse events like bomb blasts or impacts with high velocity.

The research which was done to simulate structural concrete columns, beams and slabs used the finite element program LS-DYNA in a similar way; concrete shell elements together with steel beam elements and were used to discretize the system. It is concluded that the shell/beam model is accurate enough to provide the basis for a realistic simulation of the response of a full-scale building.

The nonlinear analysis of structures was done by different researchers but most of them were on experimental. From them research done on masonry infill walls under blast loading had the x-section of infill wall shown below [8].

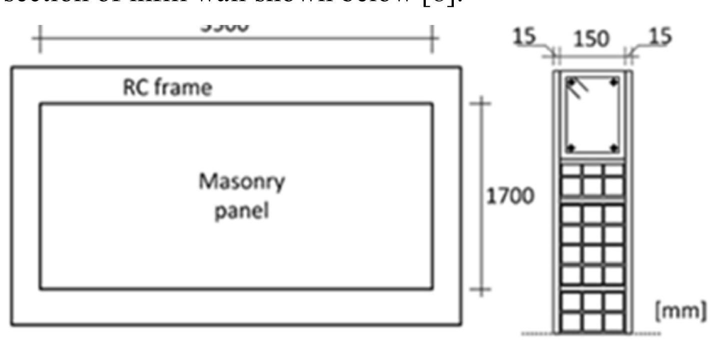

Fig.2.3a. Masonry infill Panel Schematic and geometry [8]

From the result, they concluded that there is a large concentration of large horizontal crack at the center of the wall and these spread to the corners as they move away from the center. There are also some large cracks at the top support edge, as shown in Fig.2.3b

Fig.2.3b. Damaged Wall after blast test [8]

Another research done on blast loading and effects on structures concluded that for high risk facilities, such as public and commercial tall buildings, design consideration against extreme events is very important. They also recommended that guidelines on abnormal load cases and provisions on progressive collapse prevention should be included in current building regulations and design standards. Requirements on ductility levels also help improve the building performance under severe load conditions.

Experimental investigation of structures under blast loads is difficult in our country because there are no enough equipment and instruments to do this research experimentally. So it is preferable to use finite element method.

There is very limited information available on analysis of design and detailing of structural components subject to blast loads. Research conducted on modeling and blast load effects on highway bridges reports on blast load resistant Highway Bridge, design and detailing guidelines presents some simplified design guide against blast loads. There are different researchers that investigated the response of reinforced concrete bridge columns subjected to blast loads [9].

In blast resistant design, the most effective strategy is to increase the standoff distance, because blast waves decay quite fast and increased distance results in lower pressure levels, which helps in economical design. The second major factor influencing the blast design is the provision and distribution of mass, because the weight being placed strategically helps in energy absorption under blast induced loading.

Similar to other structure bridge components could be affected by blasts. High way bridges are accessible to vehicles that can carry explosive .a finite element model of the complete bridge has been developed in one of fem analysis software called LS-DYNA. All bridge footing is constructed using solid elements and fixed boundary at the bottom and re-bars are model by beam elements. During blast loads events, the failed portion of the material needs to be removed based on maximum pressure, maximum principal stress, diavatoric stress, maximum principal strain, shear strain and impulse criterion. The maximum principal strain criterion is considered as failure criteria for materials because structural members usually have ductility and fail because of excessive displacement after yielding. The maximum impulse criterion is also another criterion for blast load effects on this research. This criterion is based on an applied impulse on the structures.it is critical when the high pressure loads occur and can predict the spalling phenomenon with short load duration.

Fig.2.3. shows the stress-time history of steel stringers under blast load.

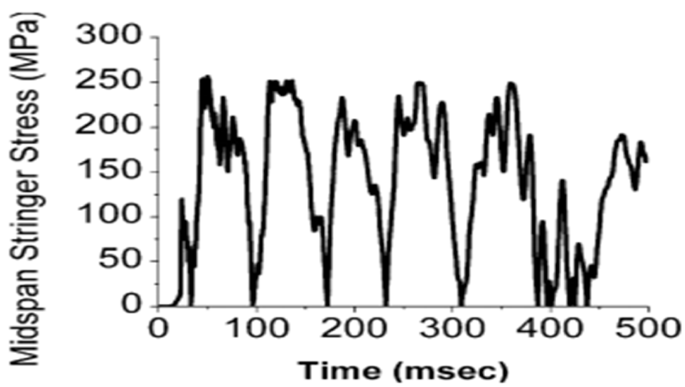

Fig.2.4. Stress time history in a stringer under blast load

It is observed that the maximum stress in a stringer reaches 259.2MPa, which is higher than the yield stress of 248.2 MPa that resulting in permanent damage to stringers.

Some researchers investigated the effects of shape of structures on blast loads. They concluded that in case of square-edge and rectangular long–edge sections, there exists almost constant peak pressures across the exposed edges and rectangular reflections near the corners of the structure. In case of the circular shape structures the highest pressure is observed at a point on the border that is nearest to the explosion and where a normal reflection occurs with decrease in magnitude toward both the sides of the center. Further shape also affects the load experienced by the structure in the event of explosion ,it is observed that a parabolic shape or a cubic shape performs better than an upright face.to provide a well-designed building, the pressure is affected by the shape of structure. Thus by analyzing the shape of a proposed building, the design can be altered to the shape that results in minimum design load and at the same provides maximum blast loading.

Similarly another research on blast load was done by pre stressed concrete institute of blast consideration shows shape of the structure can affect the overall damage to the structure of u shaped or L shaped building may trap the shock wave, which may increase blast pressure locally because of complex reflections created [9].

Test done by Fujikura and Brunea, tested a scale model of multi columns to blast loads. Test results show that the seismically designed RC and steel jacketed RC columns does not exhibit ductile behavior under blast loading [9].

2.3.1. Material Characterization

a) Concrete

Since the compression and tension stress behavior of experimental test specimens are not reported these relations are created by using mathematical models from literature. The compressive behavior of concrete is obtained by employing model along with linear descending branch.

$$\sigma = f_c\left(2\frac{\in}{\in} - \left[\frac{\in}{\in_o}\right]^2\right) \tag{2.3a}$$

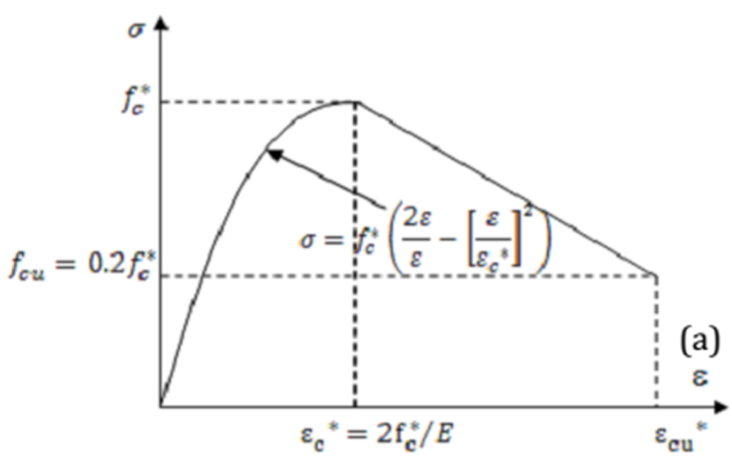

Fig.2.5. stress strain of concrete [10].

A Drucker-Prager criterion based yield function is implemented in the concrete damage plasticity (CDP) model. This function was developed with the modifications criterion based on the two stress invariants of the effective stress tensor, the hydrostatic pressure and the Mises equivalent stress represents the implemented yield function in terms of effective stresses [8].Kc is a user defined parameters that depends on the stress invariants. It must be fulfilled that 0.5≤ Kc≤1 and the factor is per default 2/3, making the yield criterion approach Rankine's formulation. The difference of the yield surfaces in the deviatoric plane for Kc=2/3 and Kc=1 is shown below. For comparison, the Rankine criterion is usually triangular whereas the Drucker-Prager criterion is circular in deviatoric plane [10].

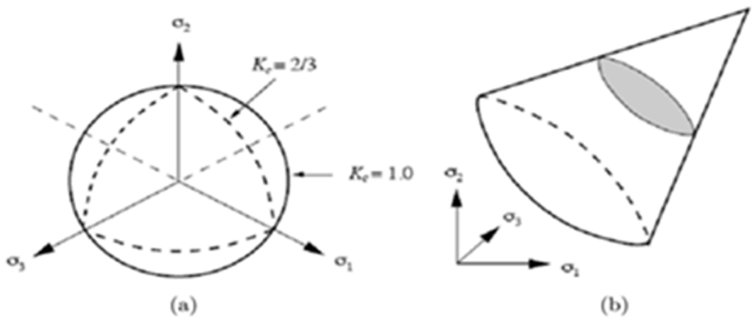

Fig.2.6. a) Drucker-Prager yield criterion in the deviatoric plane for different Kc, [10].

b) Yield surface in 3D for Kc=1 [10].

The biaxial yield surface in plane stress is illustrated on figure 2.6 below, where the enclosed area of the graph represents the elastic states of stress.to find the detailed definitions of the parameters. The connection between the yield surface and the uniaxial stress –strain relationships is determined with a flow rule.

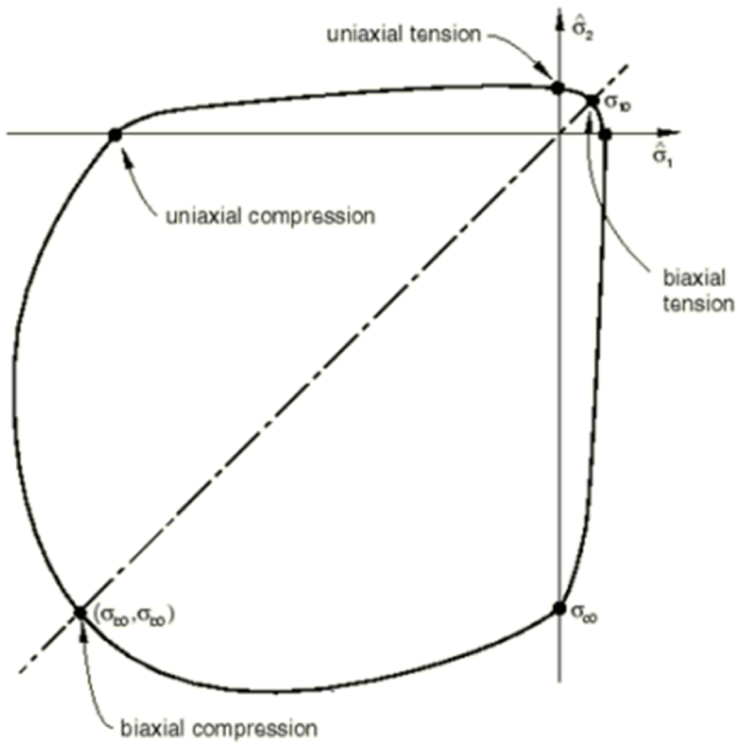

Fig.2.6c.Yield surface in plane stress [10]

In concrete damage plasticity model (CDP), the Drucker –Prager hyperbolic plastic potential function is used as illustrated in the following formulas.

$$G(\sigma) = ((\in \sigma_{to} \tan \psi)^2 + q^2)^{0.5} - p \tan \psi \qquad (2.3b)$$

Where σ_{to} is the uniaxial tensile stress at failure taken from user defined tension stiffening data and Ψ is the dilation angle measured in the p-q plane at high confining pressure. This parameter controls the amount of plastic volumetric strain developed during plastic shearing and is assumed constant during plastic yielding. Typically, the dilation angle value is selected between 30^0 and 40^0[10].

ϵ is the eccentricity parameter that defines the rate at which the function approaches the asymptote (the flow potential tends to a straight line as the eccentricity.

The central difference integration rule that was implemented in the explicit dynamic analysis is conditionally stable and can give meaningless results if the time step chosen is not short enough. Theoretically, the stability limit of an un-damped system is defined in terms of the highest frequency of the system ω_{max} [10].

$$\Delta t \leq \frac{2}{\omega_{max}} \qquad (2.3c)$$

In case of high nonlinearity, it is not computationally feasible to calculate the exact highest frequency of the system. Alternatively,estimation of stable time increment based on the shortest time interval necessary for dilatational waves to pass the elements.

$$\Delta t \leq \min \frac{L^e}{c_d} \tag{2-3d}$$

Where L^e is the length of the element and c_d the propagation velocity of dilatational waves, p-wave velocity for a linear elastic material with Poisson's ratio of zero can be calculated by following equation. Where E is the modulus of elasticity and ρ is material density.

$$c_d = (\frac{E}{\rho})^{0.5} \tag{2.3e}$$

Usually, when a more accurate representation of the higher mode response of a system is required or in problems with deformations and/or nonlinear material response, the automatically estimated time increment must be reduced.

b) Reinforcing bars

Reinforcing steel re-bars are model using beam elements or truss elements. Modeling of steel re-bars elastic plastic kinematic material model was most of the time adopted. The parameters for specifying the materials properties of steels are mass density, young's modulus, Poisson's ratio, yield strength and tangent modulus.

CHAPTER THREE

MATERIALS AND METHODS

3.1. General

The research methodology was started with identifying the sample of RC shear wall to model on ABAQUS software package and setting the objective of study. All related literature is reviewed and the background information is collected for this study.

The sample RC shear walls which can represent the shear wall type are selected to evaluate the effect of standoff distance and radial direction of loading and effect of reinforcement ratios and type of cross sectional shape of RC shear which is subject to blast (bomb) loads.

3.2. RC shear walls, reinforcement distribution, element formulation and Boundary conditions

Three sectional types of RC shear wall are considered for this study. The samples detail description of each study is elaborated below. The following, illustrates the general appearance of RC shear walls including the size shape of the sample model.

The shear walls that use to study the response using finite element analysis method for this thesis are a rectangular RC shear walls, Inverted u-shaped RC shear wall and T-Section RC shear wall types.

Type 1

1. Rectangular type of RC shear wall: the model has a size of 3060x1560x200mm.it is assumed that shear wall is restrained to translation in the bottom.

Fig.3.2a. shows the detail of a rectangular cantilever reinforced concrete shear wall which has a length (height) of 3060mm, a width of 1560mm and breadth of 200mm.

The first sample of rectangular type of RC shear wall has the center to center spacing between reinforcement bars is 300mm for the horizontal bars and center to center spacing between the vertical bars is 150mm.The reinforcement bars in both horizontal and vertical directions are calculated below.

$$h = H - (2d' + \phi) \qquad (3.2a)$$

$$No.s = \frac{(h - 2(d' + \phi/2))}{s}$$

(3.2b)

Where H = the total height of the shear wall

Φ = diameter of reinforcing bar

S = center to center spacing of reinforcing bar d' = cover of concrete

No.S = number of spacing between reinforcing bars

$No.S_h = 3000/300 = 10$ (3.2c)

Where, No S_h = total number of horizontal reinforcing bars

$N_h = 10+1 = 11$bars (3.2d)

Where, N_h is the number of reinforcing bars along horizontal direction

Similarly

$$b = B - (2d' + \phi/2) \quad (3.2e)$$

$$No.s_v = \frac{B - (2d' + \phi/2)}{s} = 1500/150 = 10 \quad (3.2f)$$

$$N_v = No.s_v + 1 = 10 + 1 = 11 bars \quad (3.2g)$$

Where:

B = total length of the shear wall

S = center to center spacing between reinforcing bars

$No.S_v$ = total number of spacing of reinforcing bars along the vertical direction

N_v = total number of reinforcing bars along vertical direction

d' = cover of concrete

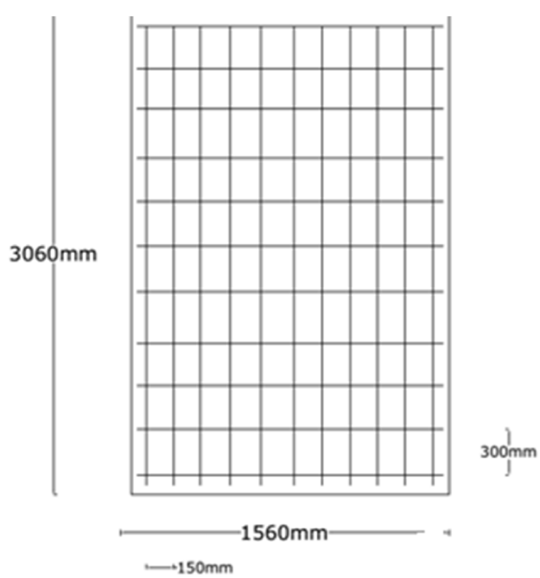

Fig.3.2a.Rectangular RC shear wall with vertical re-bar spacing of 150mm and horizontal re-bars of 300mm c/c spacing

Reinforcement ratio

Ratio of effective area of reinforcement to the effective area of concrete at any section called reinforcement ratio. For this study the reinforcement ratio is a basic element in response of RC shear wall.

Figure.3.2a. for rectangular type of RC shear wall the reinforcement ratio become:

$$\rho = \frac{A_s}{B * H}$$

(3.2h)

$$\rho = \frac{11 * \pi * \phi^2}{4 * B * H}$$

$$\rho = \frac{11 * \pi * 10^2}{4 * 1560 * 3060} = 0.0181\%$$

Where: ρ is the reinforcement ratio

As is the amount of reinforcement

B is the length of the RC shear wall

H is the height of the RC shear wall

ρ is reinforcement bars ratio

ϕ is diameter of reinforcement bar (10mm)

Figure .3.2b. Below Shows reinforcement distribution and wall dimension of rectangular type of RC shear wall with 150mm center to center spacing between reinforcing bars both along vertical and horizontal directions.

$$No.s_h = \frac{(3060 - 2(25 + 10/2))}{150} = 20 \quad (3.2k)$$

$$N_h = s + 1 = 21 bars$$

Similar to this, $N_v = 1500/150 + 1 = 11 bars$

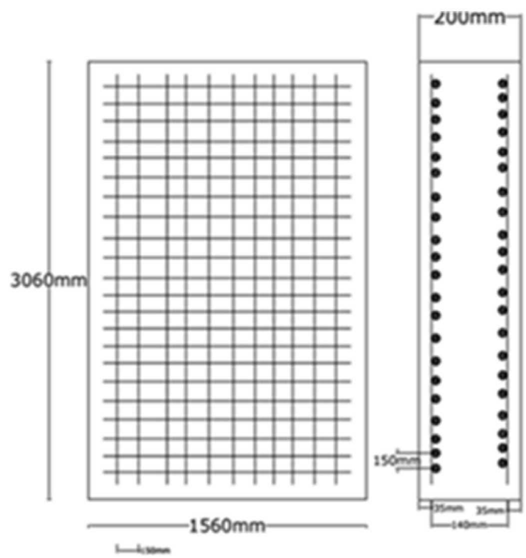

Fig.3.2b Rectangular RC shear wall sample for ABAQUS 6.13 analysis with a spacing of horizontal bars and vertical bars of c/c 150mm

Reinforcement ratio of rectangular cantilever type of RC shear wall show on above fig.3.2b

$$\rho = \frac{21 * \pi * 102}{4 * 3060 * 1560} = 0.0346\% \qquad (3.2J)$$

Type 2

2. Inverted U-shaped shear wall: the model has a size of 3060mm height, width of 200mm and length for the three sides of concrete is 1560mm. This shear wall has similar dimensional measurement to the first rectangular type of shear wall; it is restrained to the bottom.

$$No.s_v = \frac{[1560 - 2*(d' + \phi/2)]}{300} = 5 \qquad (3.2I)$$

$$N_V = No.s_v + 1 = 6bars$$

. With a similar manner,

$$No.s_h = \frac{[3060 - 2*(d' + \phi/2]}{300} = 10 \qquad (3.2m)$$

$$N_h = No.s_h + 1 = 10 + 1 = 11bars$$

The three sides of Inverted u-shape reinforcement bars have the same diameter of bar and the same number of bars. For the two directional re-bars the diameter of re-bar is 10mm and 25mm cover of concrete.

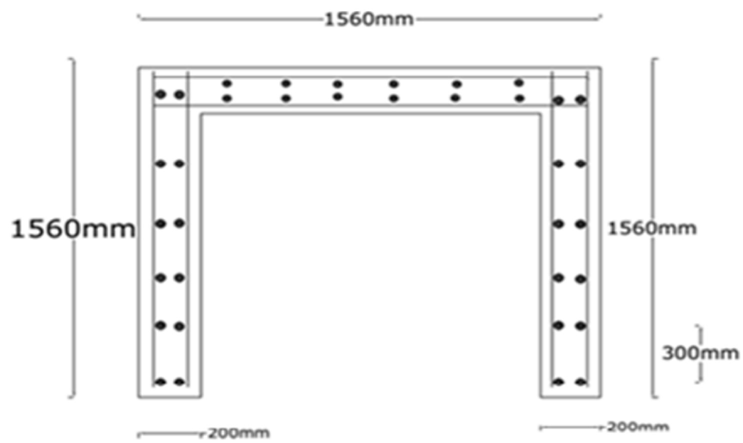

Fig.3.2c Inverted U-shaped RC shear wall sample for modeling on ABAQUS 6.13

Type 3

3. T-Section reinforced concrete shear wall: the model has a size of 3060mm height; width of 200mm and the three sides of concrete is 1560mm similar to other section like Inverted U-shaped RC shear wall and rectangular cantilever type of shear wall. It also restrained at bottom to translation. The numbers of reinforcement bars are calculated with a similar manner to the above type of RC shear walls.

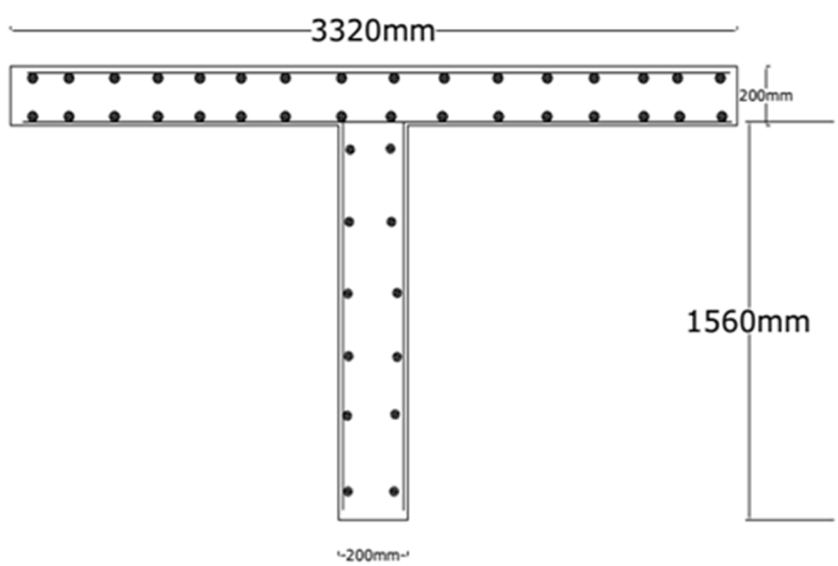

Fig.3.2d Model of the T-section RC shear wall

3.3. Description of the model

In developing advanced analysis of reinforced concrete shear wall subject to blast loads (bomb) procedures, the common approach has been to first model a structure that is create parts for concrete and vertical bars and horizontal bars separately one by one, create material definition for each materials, for concrete and steel bars and assemble the parts as the unit model, and then to implant some analysis method like finite element analysis (numerical simulation) method to analyze. There are two inherent parts modeling of reinforced concrete shear wall and analyze by using a finite element method in case of applied bomb. First, the RC shear wall modeling is usually based on materials properties that to capture the model. Secondly, the analysis is done under bombs are considered and formulate the response of the structure or study the behavior of RC shear wall.

3.3.1. The flow chart of modeling of RC shear wall on ABAQUS 6.13 procedures

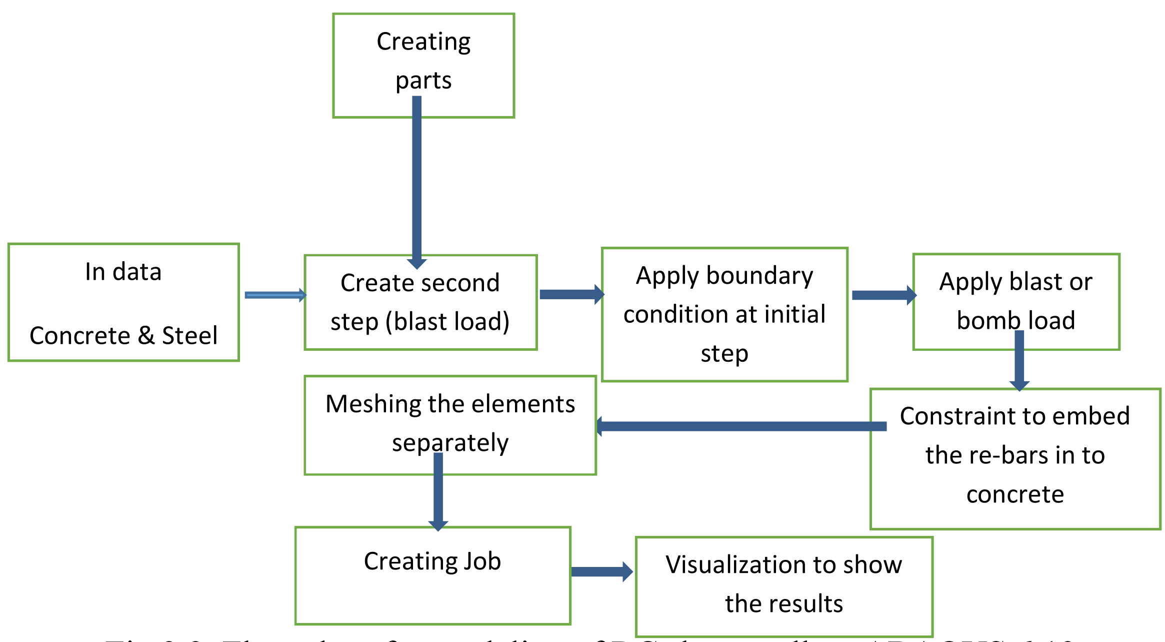

Fig.3.3. Flow chart for modeling of RC shear wall on ABAQUS 6.13

3.4. Concrete and re-bar materials

In order to develop a nonlinear finite element model of reinforced concrete shear wall under bomb load in computer simulation of ABAQUS package, it is important to select proper material constitutive formulation for structural components. The following materials are got from European standard. Euro code 2: design of concrete structures part 1 on section 3 the concrete materials and reinforcing steel material are described with detail requirements.[7]

Concrete: from table 3.1. Stress and deformation characteristics for concrete, for C20/25 concrete strength the value of elastic modulus of concrete, E_C=30GPa and Poisson's ratio equal to 0.2 for un cracked concrete and 0 for cracked. Therefore the Poisson's ratio is between 0 and 2.

Using similar standard code,european stanadard code, the steel materials has the mean value of density become 7850kg/m^3 and poisson's ratio of 0.3 is given.

For simulating the reinforced concrete shear wall model ABAQUS 6.13 material type C3D8R, which is an 8 nodes linear brick, reduced integration hourglass control use for formulation of concrete element as solid element. It takes reduced integration by using a low-order integration (eight integration points) to form the elements stiffness matrix that will reduce running time with 3D stress element formulation. The mass density of concrete is set to 2.4x10^{-9}Mg/mm^3, the Poisson's ratio of concrete of 0.2, the young's modulus of concrete set to 30000MPa.From the material module of ABAQUS there is mechanical property, under the mechanical property there is plasticity, compressive and tensile parameters that shows a general behavior of concrete. Plasticity property of concrete is defined by concrete damage plasticity.

Concrete damage plasticity (CDP) model in ABAQUS/Explicit provides the ability to model the behavior of plain or reinforced concrete elements subjected to dynamic loads. The model uses concepts of isotropic damage plasticity to represent the inelastic behavior of concrete i.e. tensile cracking and compressive crushing.

In ABAQUS the parameters required to define plastic property of concrete is concrete damage plasticity model.

Therefore, using CDP model enables a proper definition of the failure mechanisms in concrete elements.The CDP can be used to model the behaviour of concrete structures in adavanced states of loading.Based on the criterion defined and application of CDP model of concrete.The study also serves as a link between the real behaviour of concrete and its numerical modeling

Concrete damage plasticity model, uses the isotropic damage plasticity in combination with isotropic tensile and a compressive plasticity to represent the inelastic behavior of concrete.

Concrete damage plasticity model is designed for application in which concrete subject to cyclic loading with alternating tension compression loading like seismic problems and blast load problems.

Concrete damage plasticity model does not allow the removal of elements during the analysis. This CDP model does not contain a failure criterion.

The plastic material property of concrete taken as concrete damage plasticity behavior has the following parameters;

1. The Poisson's ratio (V), it controls the volume changes of concrete for stresses below the critical values which is onset of inelastic behavior.
2. In concrete damage plasticity model (ψ) is dilation angle measured in pressure vs q plane at high confining pressure.
3. Eccentricity (ϵ) of the plastic potential surface is also main parameter in concrete damage plasticity model
4. The ratio of initial biaxial compressive yield stress to initial uniaxial compressive yield stress (σ_{bo}/σ_{co}).
5. Ratio of the second stress invariant on the tensile meridian to compressive meridian at initial yield (K_c).

Table3.1. Four input elements of concrete damage plasticity with their values

Poisson's ratio(V)	0.2
Dilation angle(ψ)	31^0
Eccentricity(e)	1.10
σb0/σco	0.1
Kc	0.667
Viscosity Parameters	0

The plastic behavior of concrete is developed by using the given stress with strain related equation for estimation of uniaxial stress-strain curve,

$$\sigma = f_c\left(\frac{2\in}{\in} + \left(\frac{\in}{\in^*}\right)^2\right) \qquad (3\text{-}4a)$$

Where, σ= total stress of concrete

Є=total strain of concrete

$\epsilon^*=2\,{}^{0}\!/_{00}$

f_c=25MPa

Inelastic strain =total strain –stress/E_c

E_c=30MPa

Table3.2.1. Stress-strain values for compressive behavior

Stress	total strain	inelastic
0	0	0
5	1.125E-07	0.00016655
9	1.025E-07	0.0002999
12.5	9.375E-08	0.00041657
15.5	8.625E-08	0.00051658
17	8.25E-08	0.00056658
18.5	7.875E-08	0.00061659
20	0.000000075	0.00066659
21.5	7.125E-08	0.0007166
22.5	6.875E-08	0.00074993
23.5	6.625E-08	0.00078327
24.5	6.375E-08	0.0008166
25	6.25E-08	0.00083327
25	6.25E-08	0.00083327
24.5	6.375E-08	0.0008166
24	0.000000065	0.00079994
23	6.75E-08	0.0007666
22	0.00000007	0.00073326
21	7.25E-08	0.00069993
20	0.000000075	0.00066659

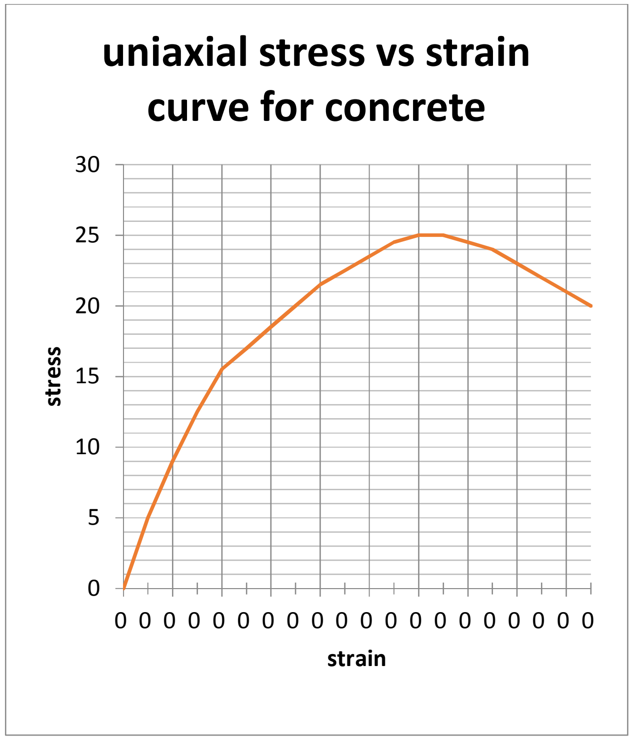

Fig.3.4a. stress strain compressive behavior of concrete

On ABAQUS, stress and inelastic strain is one of the basic inputs under compressive behavior of concrete for concrete damage plasticity model. Similarly, the tensile behavior of concrete also inserted under tensile behavior of concrete damage plasticity model

Table3.2.2. stress, total strain and inelastic strain for tensile behavior of concrete

Stress	**total strain**	**in elastic strain**
0	0	0
2.25	0.00011	0.000035
1.4667	0.00033	0.00028111
0.825	0.00065	0.0006225
0.3667	0.00116	0.00114778
0	0.00176	0.00176

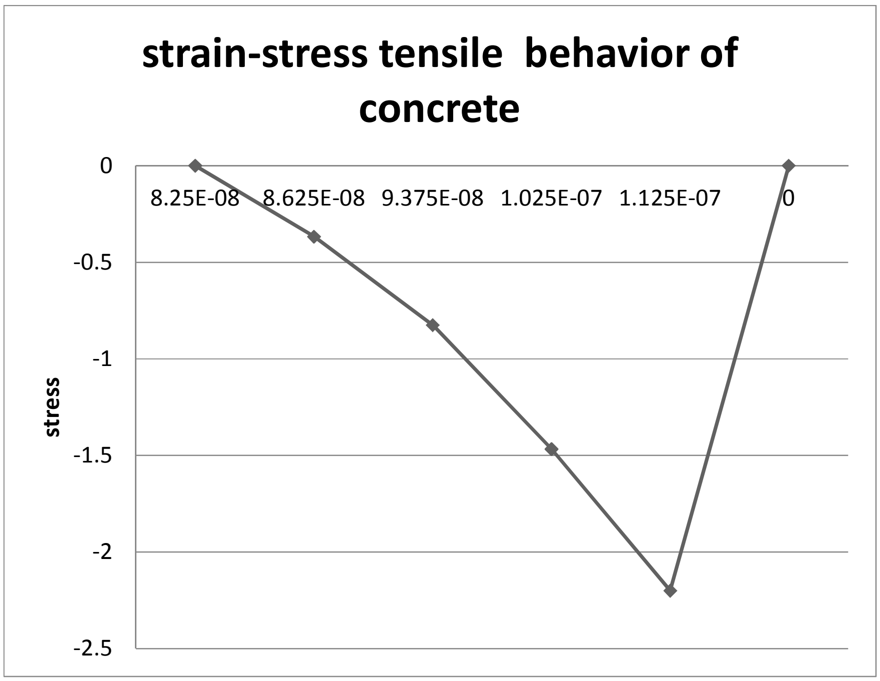

Fig.3.4b. tensile stress –strain graph of concrete

As the uniaxial behavior of material models defines the evolution of the yield criterion in a finite element analysis,the definition of material parameters and uniaxial material behaviour curves becomes more important.

Steel bars model using line element as truss element with T3D2 element formulation, a general purpose linear A2 nodes 3D truss element type for simulation. The density of bar is $7.85x10^{-9}$ Mg/mm^3, young's modulus of steel bar set to 210000MPa, the Poisson's ratio of steel bars is 0.3, yield stress of steel bar is 350MPa and inelastic strain of steel equal to 0.The assumed time period for explicit description of bomb load set to 0.001sec for explicit analysis of all rectangular, inverted u-shape type of RC shear wall and T-section RC shear wall. Explicit is used to analyze the dynamic effect of structures.

3.5. Load

3.5.1. Bomb load

Bomb is one of solid physical type of blast load. Blast load is a sudden release of energy as surface burst and as air pressure. Bomb loads have an impact on the life of peoples and property damage. The event which occurred in our country Ethiopia during derg regime (Socialism Empire) was main event that was the reason for many people's death and loss of their properties. Most of the time the bomb load consideration was given for structure which is found around military area and things that are located around military area. But now a day there are many events happened in civil structures. As a wittiness, the event that were happened on public building which located at New York City on September 11th, 2001 on world trade center. This shows design and analysis consideration of bomb loads for any structure that found on any areas not only military areas must be considered.

There are different methods to apply blast load on the structure which are vehicle bombs, motorcycle bombs or hand bombs to apply on target point. Vehicle bomb are bombs which are placed on vehicles to explosive purpose. Motorcycle bombs, bombs are placed on motorcycle for explosion and hand bombs are bombs that are applied by putting on ground surface or throw it to target location. For this study hand bomb which is place on ground at different distance and at different radial direction. To know the response of hand bomb which is placed on ground, distance from location of bomb to target point, orientation of bomb location and amount of bomb mass weight are the main elements for load effect on structures. ABAQUS present ways to apply blast (bomb) load pressure to RC shear wall generally for all structure. The blast load or bomb can be provided by the load command of ABAQUS. This load command provides page to input information. The charge weight, distance of bomb from the target point (shear wall) called standoff distance are used to define the magnitude of bomb loads. The bomb load is TNT. Close in is the distance between the target location and blast or bomb location is within very short distance, similar to this the distance target to bomb location increased to be far field and distance between target location and bomb is near to each other called near field.

According to Smith, the scale distance, Z which is defined as the ratio of standoff distance to cubic root of charge weight, determine the location of bomb or blast load from the target location.

Close in: $z < 1190\, mm / \sqrt[3]{kg}$

Near field: $1190 < z < 3967\ mm\Big/\sqrt[3]{kg}$

Far field: $z > 3967\ mm\Big/\sqrt[3]{kg}$

For this study, there are three load cases. Close in bomb is the first load case applied as pressure loads with a given time period and amplitude. Close in is the distance between the RC shear wall location and the bomb location that placed on ground become very close to each other. Similarly the far field means the distance between location of bomb and the RC shear wall structure location is large and near field case, the bomb location to RC shear wall distance is small.

The bomb load which has 5kg mass size as a pressure loads is applied at different standoff distance and at different radial directions. The standoff distance consider for analysis of the three RC shear wall are 1m standoff distance that is close in case, 3m standoff distance near field, 7m standoff distance far field and 11m standoff distance which is also far field.

Load case 1: close in bomb

The close in load is very close to the RC shear wall.in this case, standoff distance ,R, is 1m and charge weight w, set to 5kg.Hence the scale distance become, $z = 693.36\ mm\Big/\sqrt[3]{kg} < 1190\ mm\Big/\sqrt[3]{kg}$

An expression which is presented by Mills for pressure calculation is

$$p_{so} = \frac{1772}{z^3} - \frac{114}{z^2} + \frac{108}{z} \tag{3.5a}$$

Where: p_{so} is peak over pressure of bomb and Z is the scale distance.

$$p_{so} = \frac{1772}{693.36^3} - \frac{114}{693.36^2} + \frac{108}{693.36}$$

$p_{so} = 0.15553kPa$ Or $155.53Pa$

Load case 2: Near Field Bomb

The near field case, the standoff distance is 3m and size of bomb is 5kg.Therefore the near field has a scale distance between 1190< Z<3967 $mm\Big/\sqrt[3]{kg}$.

For the standoff distance 3m and size of bomb 5kg, the scale distance become 2080.08 $mm\Big/\sqrt[3]{kg}$ and the pressure distribution of bomb load is 51.89 Pa.

Load Case 3: Far Field Bomb

The far field case needs a high standoff distance. The RC shear wall subject to far field TNT occurs when the scaled distance, $z > 3967\, mm / \sqrt[3]{kg}$.

This give the standoff distance of 7m, 11m and bomb weight size is 5 kg.

With a similar manner to load case 1, load case 2 pressure loads also determined by using above peak over pressure load expression

$$p_{so} = \frac{1771}{z^3} - \frac{114}{z^2} + \frac{108}{z} \tag{3.5b}$$

The pressure bomb load for 7m standoff distance is 22.25 Pa and for 11m standoff distance the bomb load is 13.62 Pa

Since, the standoff distance for close in case is lower than the far field load case and the pressure for close in has a higher pressure load than the far field case. Thus, the peak pressure increases, the standoff distance decreases.

Table3 3.3. Amplitude- time table

Time	Amplitude
0.00001	0
0.0001	100
0.0002	100
0.001	0

3.5.2 Orientation of bomb load

The location of bomb is an important factor in amount of energy dissipated to the RC shear walls. In this study, the blast or bomb load considered as pressure load and it is placed at radial direction at different standoff distance from the RC shear wall. The figure below shows the location of bomb load from RC shear wall at 1m, 3m, 7m and 11m standoff distance radially. The first location of bomb is when the load placed in front of the RC shear walls and the second one when the bomb is placed on the side of Inverted RC shear wall or on the side location of the T-section RC shear wall. The third location of loading is at the back of Inverted u shaped RC shear wall or at the back of T-section RC shear wall. Generally to study the response of RC shear wall, the location of bomb loads are radial location 1, radial location 2 and radial location 3 with different standoff distance which are listed above.

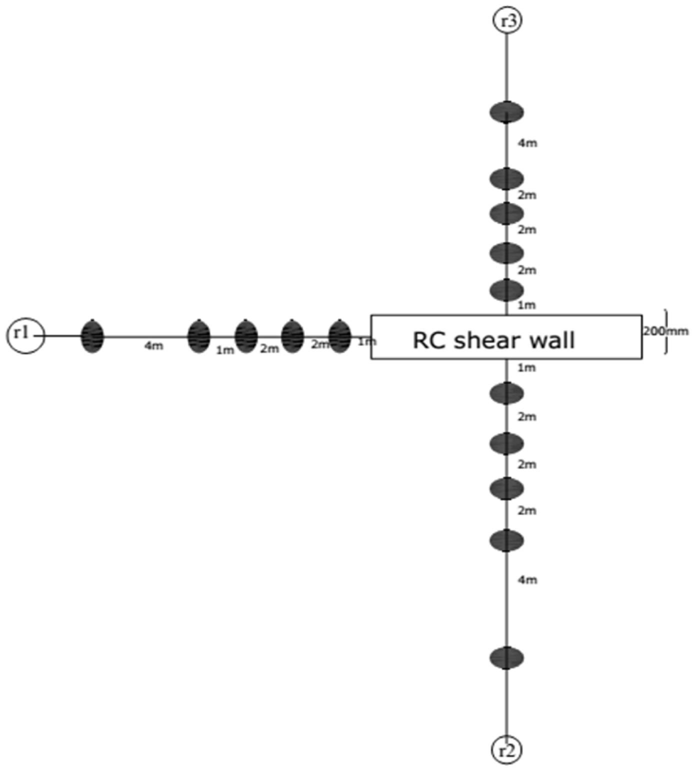

Figure3.5.1 Different standoff distances and radial directions of bomb loads.

3.6. Boundary condition

The bottom part of RC shear walls or all bottom nodes are restrained against translation. The applied restraint creates a fixed boundary condition. Therefore, this restraining condition develops a fixed support.

For a rectangular cantilever shear wall, the boundary condition for the initial step is fixed at the bottom. Similar manner the inverted u-shape of RC shear wall and T-section RC Shear wall also have fixed support at bottom parts of three sides.

The figures below show the fixed support and the bomb load distribution for different radial directions and for different standoff distances. This study uses three radial directions of loading. Radial direction 1 Which bomb load is placed in front of RC shear wall at different standoff distance, radial direction 2 that placed on side of RC shear wall with a given standoff distances and radial direction 3 that bomb locate at different standoff distance on the rear of RC shear walls.

Figure **3.6.1, 3.6.2** and **3.6.3** shows the radial direction 1 case of bomb loading i.e. in front of each reinforced concrete shear walls at 1m, 3m, 7m and 11m standoff distance.

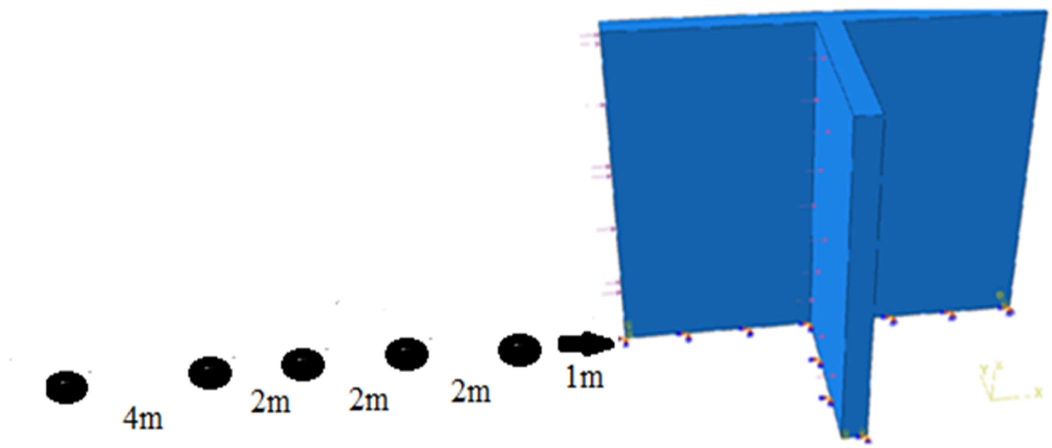

Fig.3.6.1. Boundary condition and bomb load distribution of T-section RC shear wall

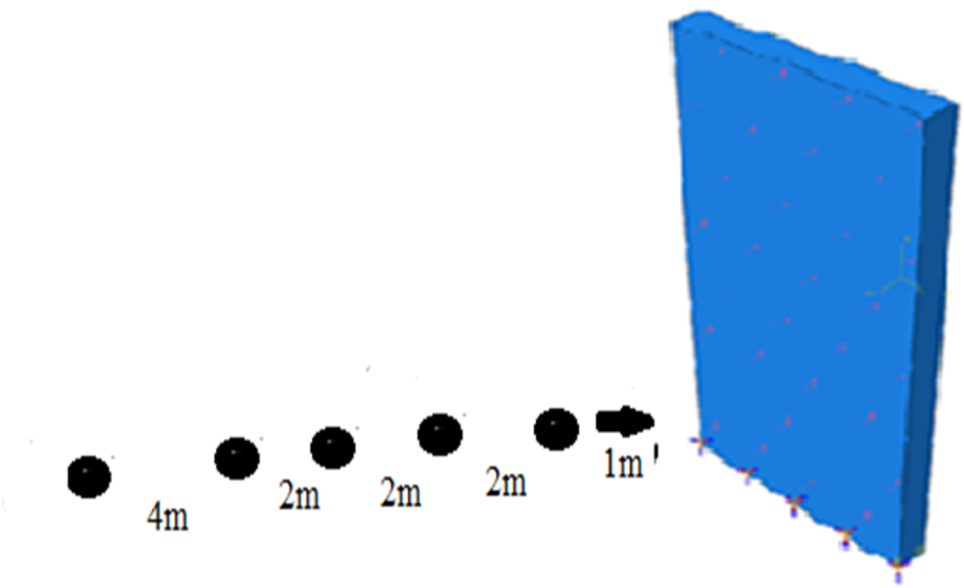

Fig.3.6.2. Boundary condition and bomb pressure load of rectangular RC shear wall

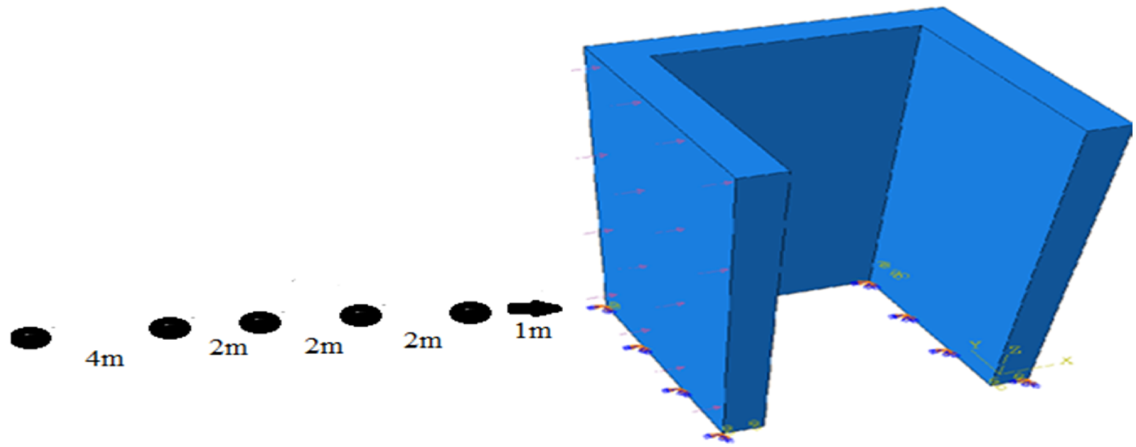

Fig.3.6.3 Boundary condition and bomb distribution of Inverted u-shaped

The Figures below shows the boundary condition and bomb load distribution for second bomb location case that is radial direction 2. Bomb pressure load applied on the side of RC shear walls.

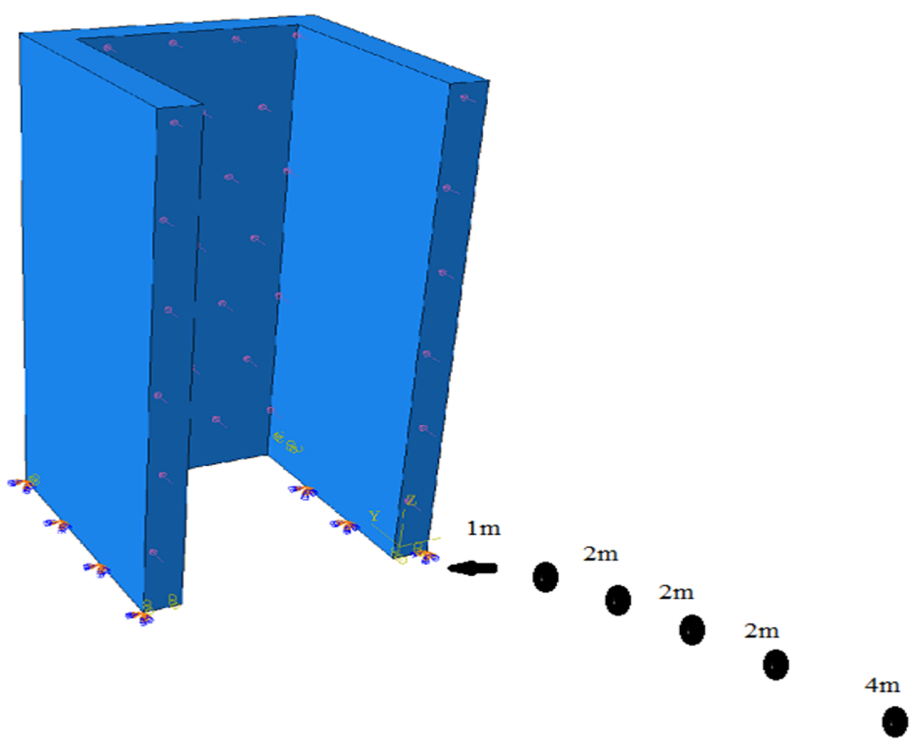

Fig.3.6.4. boundary condition and bomb pressure load distribution for location 2 case

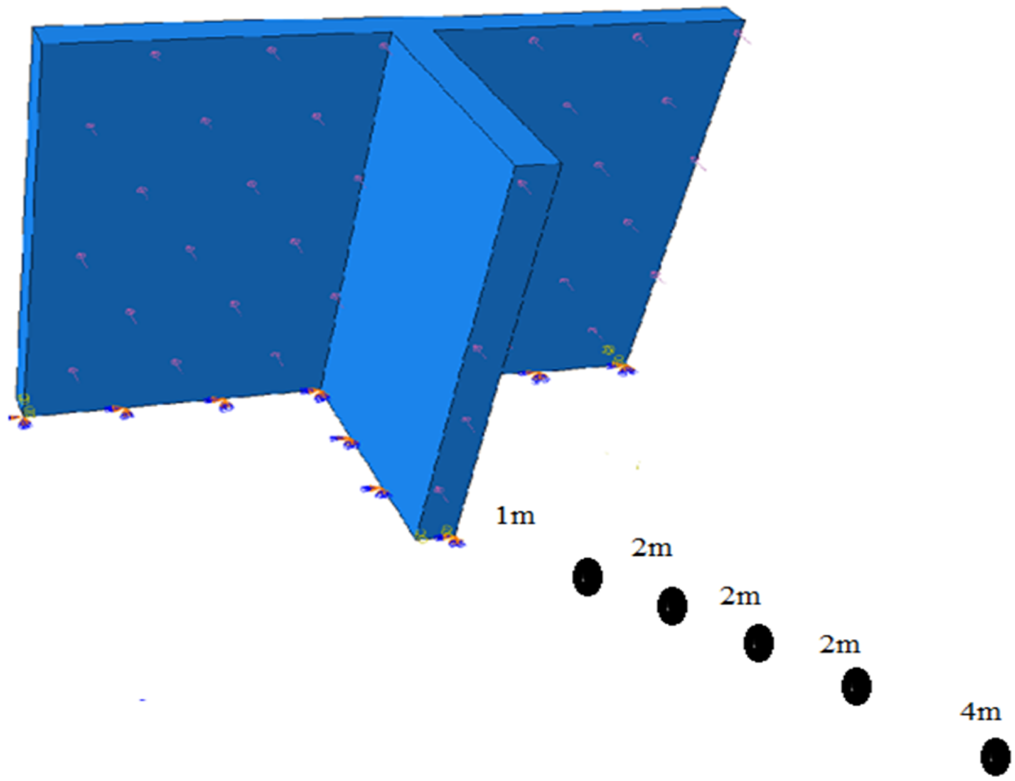

Fig.3.6.5. Boundary condition and bomb pressure load distribution for location 2

The figures shown bellows are boundary condition and radial direction3 bomb load location.

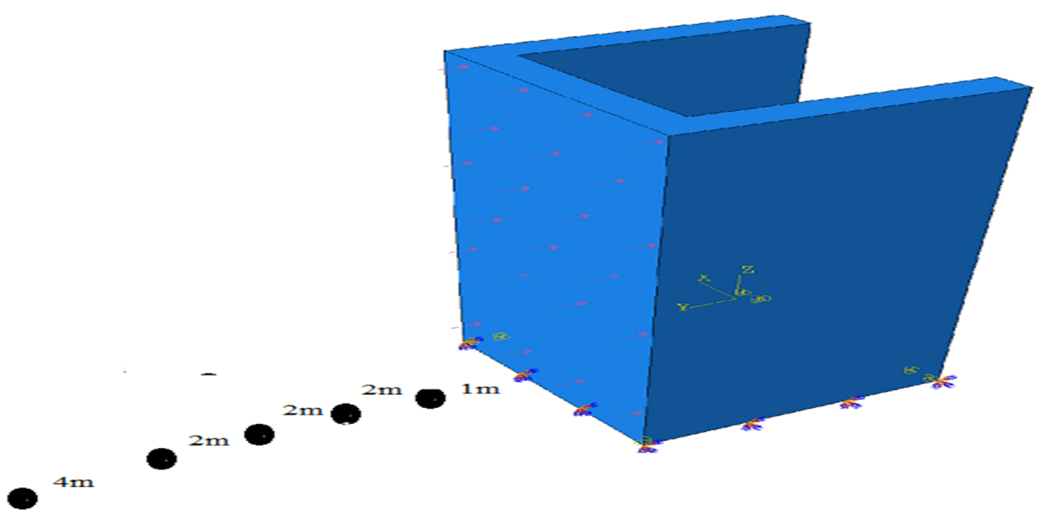

Fig.3.6.6. Boundary condition and bomb loading for different standoff distances

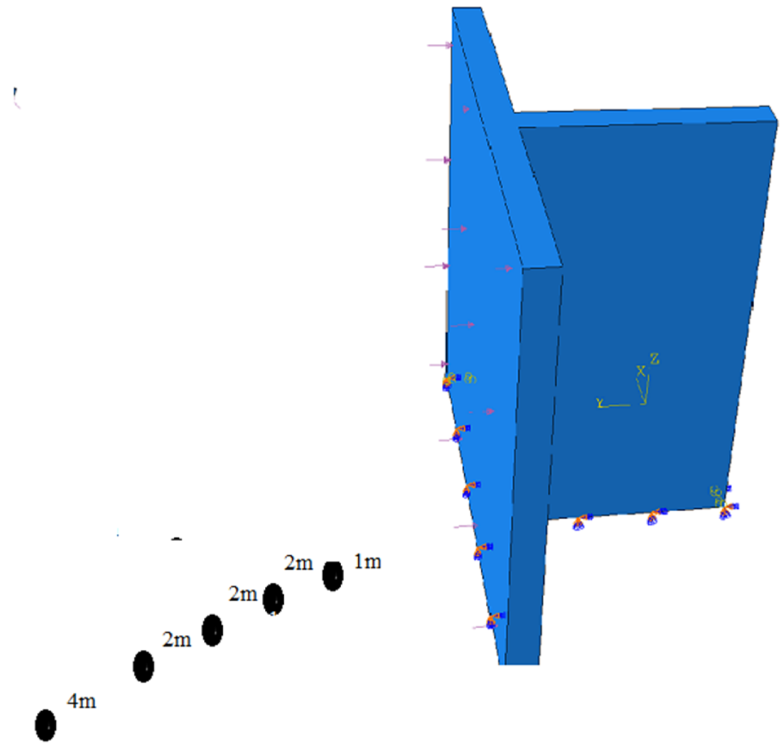

Figure 3.6d Boundary condition and radial direction 3 load distribution

3.7. Mesh Size and Element Type

Most researchers agree, mesh size has an effect on finite element analysis of different reinforced concrete structures. Related to this the accuracy of the finite element analysis depends on the mesh size of. According to this the finite element is finer or smaller the structural response on finite element.

The numbers of investigation were done the effect of mesh size on the result of finite element analysis of structure. Different results obtained for different mesh size and the accuracy of the response could close, when the nodes of the structure increase.

The finite element mesh was consists of solid elements for the concrete wall and the steels reinforcements were modeled by linear elements (truss elements).

This study consists of 80mm mesh size for rectangular cantilever type of RC shear wall. The first one is rectangular cantilever type of RC shear wall have 80 mesh size for each parts means concrete part and reinforcement bars part for each reinforcement configuration.

For this case of meshing 80mm mesh size, the horizontal bars are generating 399 elements, the concrete wall part consist 2280 elements and a vertical bars generate 418 elements.

The next type of RC shear wall is inverted u-shape of RC shear wall. For this type of RC shear wall, the mesh size use for the purpose of meshing is 80mm uniform mesh size.

The rectangular type of RC shear wall having a reinforcement ratio of 0.018% with a mesh size of 80mm give 209 elements are generate for horizontal bars, 418 elements for vertical bars and 2280 elements are generate from the concrete part of RC shear wall.

The Inverted u-shape RC shear wall also contains 3 times 209 elements of horizontal re- bars, 3times 60 elements of vertical re-bars and a total of 6308 elements for Inverted u-shape of concrete part.

The complete model consists of 80mm mesh size case. The truss elements used for modeling of reinforcement bars were embedded in solid concrete wall element through the term constraint that provided perfect bond between the re-bars and concrete. The following figures shows some mesh sizes of the 3 types of RC shear wall with 80mm mesh size

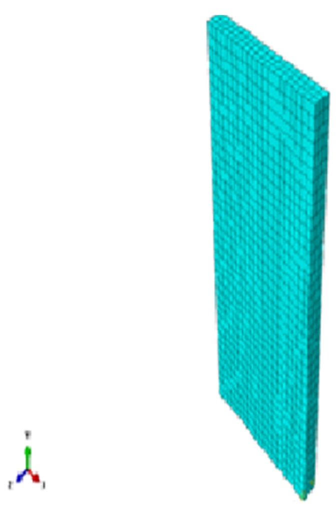

Fig. 3.7a) mesh of cantilver rc shear wall

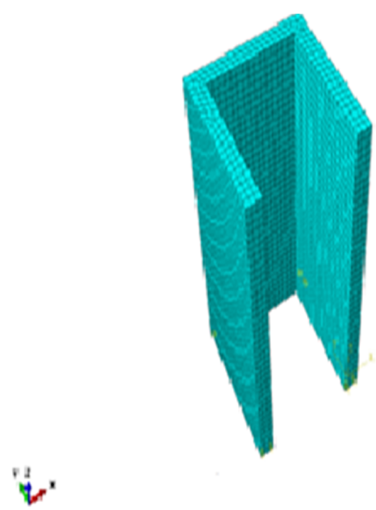

Fig.3.7b) mesh size for Inverted u shaped RC shear wall

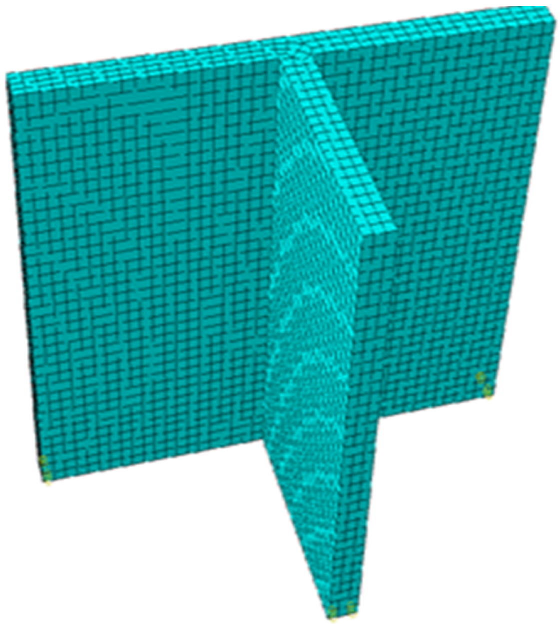

Fig.3.7c) Mesh of T-sectional RC shear wall

CHAPTER FOUR
VALIDATION OF FINITE ELEMENT MODELING

4.1 Validation of the Results

This section present the research which was done by researcher called Shetye et al. , the response of RC slab which is subject to blast loads to ensure the validity of the result of blast loads response on RC shear walls. As given element which were given on research, the slab was tasted under a blast load of 5kg weight.The aim of this research is to study blast load response of different types of one way RC slabs. The slabs include high strength concrete with high strength steel material combination and normal strength concrete with normal strength steel material combination and also has different reinforcement ratios. Research was done both numerically and expermentally. Expermental result obtained from tests conducted on 12 RC slab panels in blast load simulator with geometrical size of slab 1652mm x 857mm x 101.6mm dimension that had 101.6mm main steel spacing on center with two end bars at 50.8mm spacing and transverse steel, shrinkage steels had 304.8mm spacing on center.

The tewleve slab panels consist of two reinforcement ratios 0.68% and 0.46%. Finite element models of 12 slabs are developed in ABAQUS 6.13 analysis Software.The blast pressure applied on the experment also applied with the same pressure load magnitude on numerical simulation. The concrete models available for material combination response to blast loading is studied using C3D8R to account damage effects with plastic kinematic steel model and this study used constrained in solid to model bond between concrete and reinforcement steels. The basic input datas used for numerical simulations are material property of concrete used concrete with a density of 2409kg/m^3 , 24.8GPa concrete intial tangent modulus, 0.18 value of poisson's ratio , uniaxial compressive stresngth of 80Mpa, uniaxial tensile strength of 6.4MPa.

The Steel material properties used for steel modeling are mass density of 7830kg/m^3, Young's modulus of 200GPa, poisson's ratio of 0.3, Yield strength of reinforceing steels of 572.26MPa [11]. This material parameters are present on the following table

Two mesh sizes of 25.4mm and 12,7mm mesh sizes with different reinforcement ratio used on response for slab.The 25.4mm mesh size model has 11,375 nodes and 8704 solid elements.The total number of beam elements for 101.6mm spacing with 25.4mm mesh size is 746 elements.The boundary condition for modeling of slab is all sides along Y restrained.

The RC slabs dynamic response was recorded as center span displacement with respect to time. The displacement time history measured using laser deflectometers in experment where used for comparision with numerical model developed for different mesh sizes in this study. Comparision was done for high strength concrete with high strength steels with 0.46% reinforcement ratios and 25.4mm mesh size.

The following graph presents the comparision results obtained from numerical simulatin of salb with 20mm mesh size and 80mm mesh size to 25.4mm mesh size result which was obtained from numerical result of RC slab for 0.46% reinforcement ratio and expermental result for the same geometry of slab that was done on response of slab for 5kg blast loading. Defelection is the main criteria which used for comparision of the result of analysis result with expermental results. On the following graph, Expermental deflection recorded plot on the following graph and the numerical study results also present to take the peak deflection values for comparision of mesh size effect for different mesh sizes.

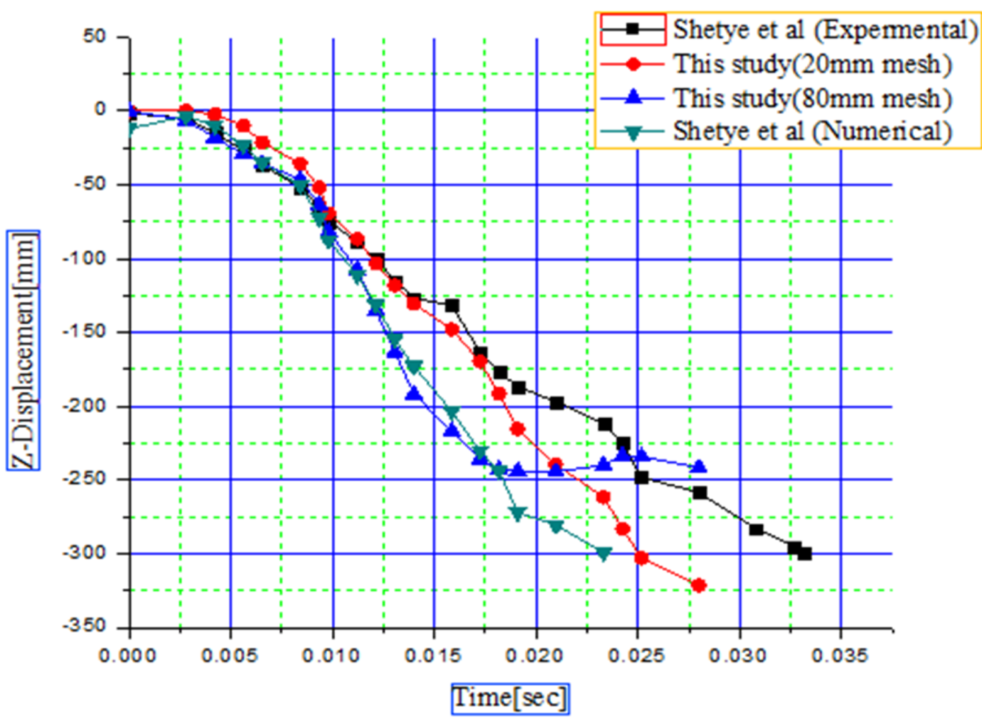

Fig.4.1a. Deflection comparison of CDM3 model of RC slab for 25.4mm mesh and a mesh size of 20mm and 80mm with Experimental result

The above graph displacement time history curve shows the displacement distribution for the 3 types of mesh size and experimental result of RC slab which was given by researcher. Peak deflection values for these different mesh sizes used for comparison of mesh effect on slab structure subject to blast load of 5kg TNT bomb.

The figure predict the peak deflections for numerical result of 25.4mm mesh size is 299mm As shown on the graph for mesh size of 20mm mesh size the peak deflection was around to 321mm, whereas the mesh size was 80mm size, the peak displacement has an approximate value of 241mm and experimental validation of RC single mat slabs subject to blast research result shows the peak value of deflection equaled to 300mm. Therefore the result predicted for higher mesh size, produced lesser deflection and also figure predict the peak deflection of 25.4mm mesh size numerical result more closely to experimental but the mesh size increase to 80mm mesh size the deflection drop from 300mm experimental result to 241mm for mesh size of 80mm.

CHAPTER FIVE

RESULT AND DISCUSSION

5.1. Results

The following results are drawn using an integrated element and unique nodal on ABAQUS from analysis output on visualization command of ABAQUS version 6.13 Software. All result of displacement time history graph read at the central nodal point of RC shear wall and for all type of RC section the nodal point used to extract deflection time graph data are the same node. The data used to draw stress strain graph and stress time history graph are taken from the central integrated point of each RC shear walls.

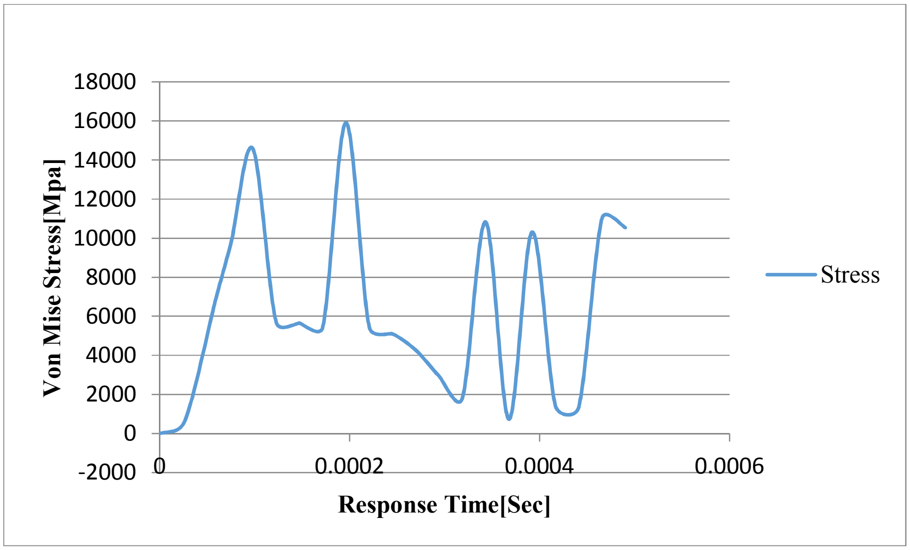

Fig.5.1a.Mise Stress- time curve for rectangular cantilever RC shear wall with 80mm mesh size and 1m standoff distance at radial direction 1

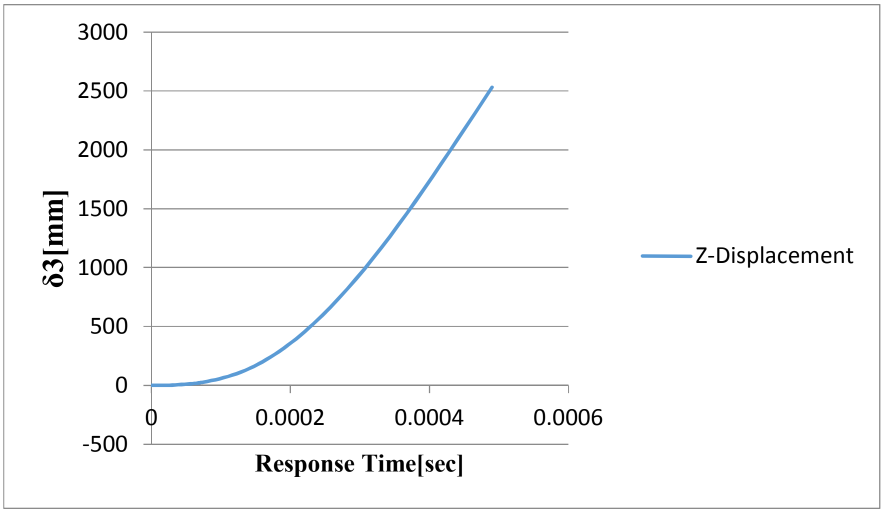

Fig5.1b. Displacement-Time History curve of Rectangular RC shear wall at 1m standoff distance and front load location.

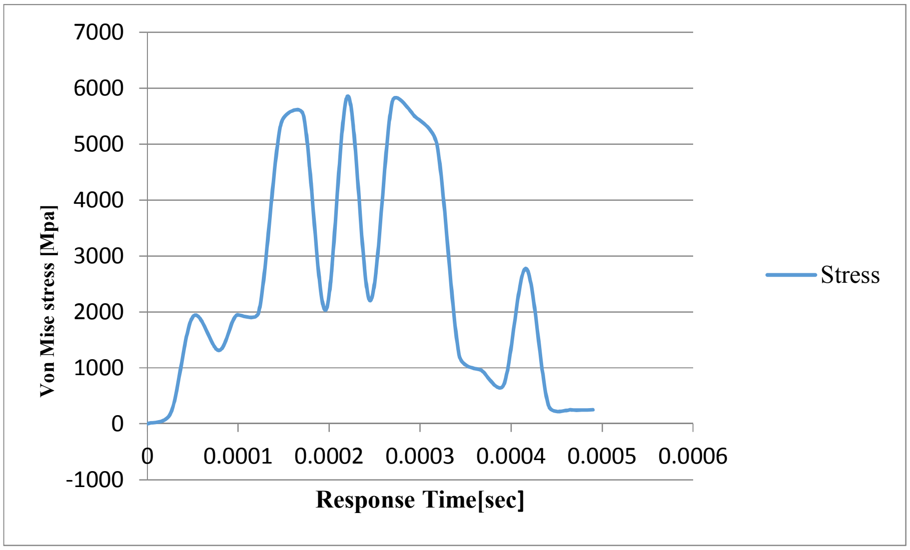

Fig.5.1c. Mise stress-time of Rectangular RC Shear wall at standoff distance 3m and radial direction 1

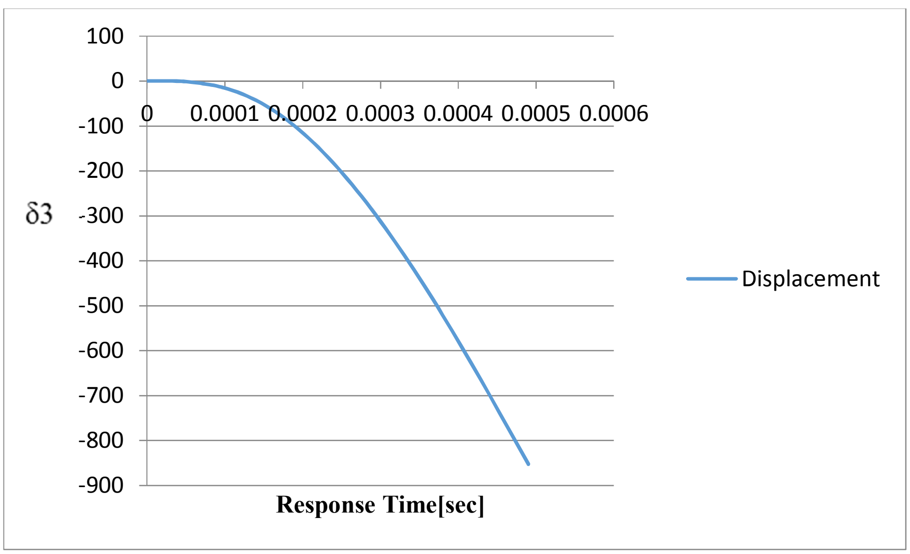

Fig.5.1d. Z-displacement at 3m standoff distance and at front of Rectangular RC shear wall

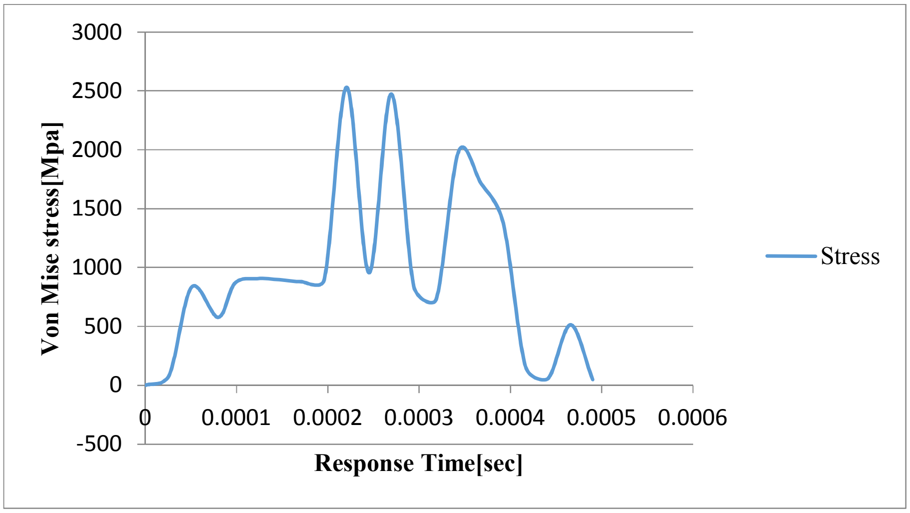

Fig.5.1e. Mise stress Time history curve of 7m standoff distance and front bomb load location

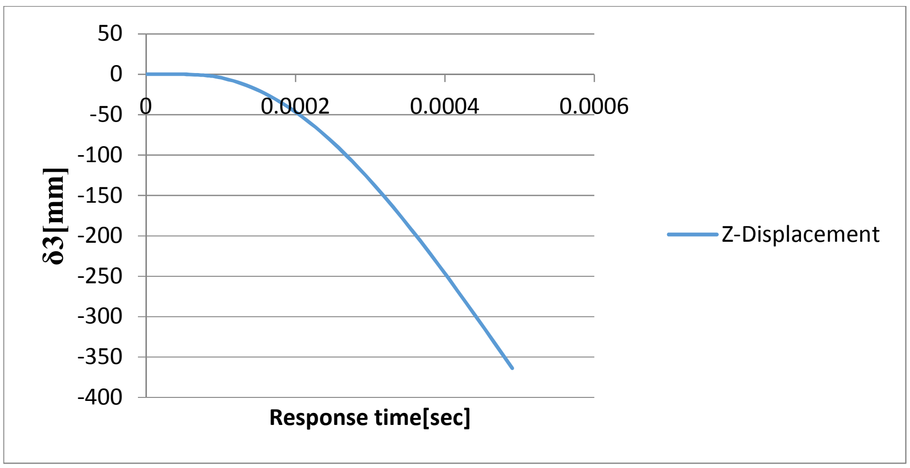

Fig.5.1f. Z-displacement Time history curve of 3m standoff distance and front location of bomb load of Rectangular RC shear wall

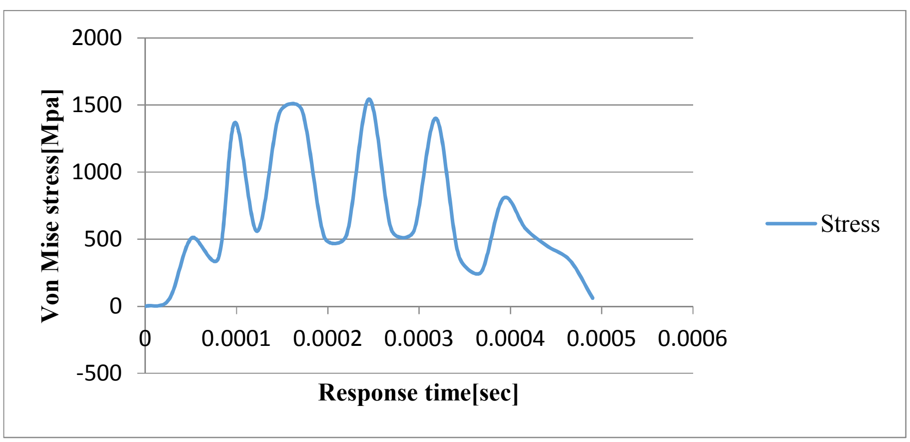

Fig.5.1g. Mise stress- time history of Rectangular RC shear wall at 11m standoff distance and front location of loading

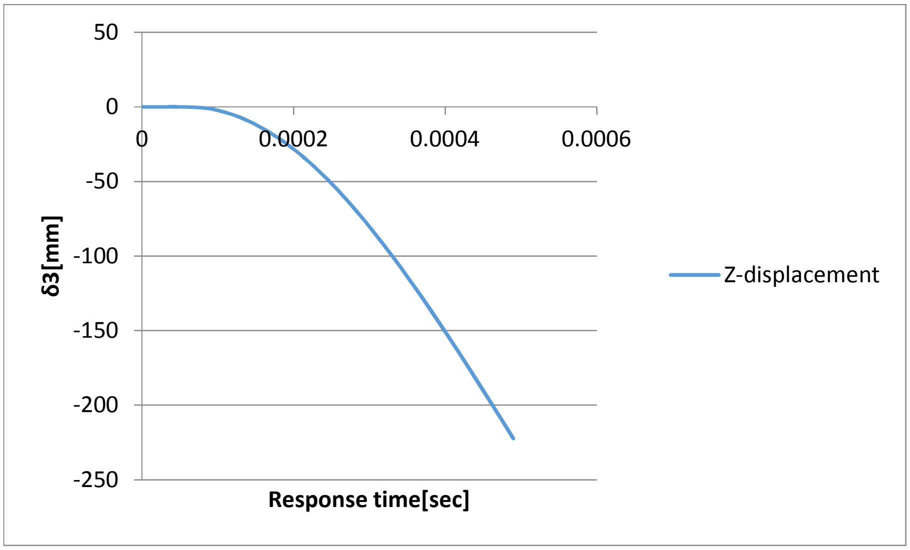

Fig.5.1h. Z-displacement –Time history curve of Rectangular RC shear wall at 11mm and front location of bomb load.

Similar to the above stress and displacement distribution of rectangular RC shear wall also the T-section and Inverted U shaped analyze using 1m,3m, 7m and 11m standoff distance and radial direction 1 that load is placed in front of RC shear wall for the given stand of distances are shown bellows.

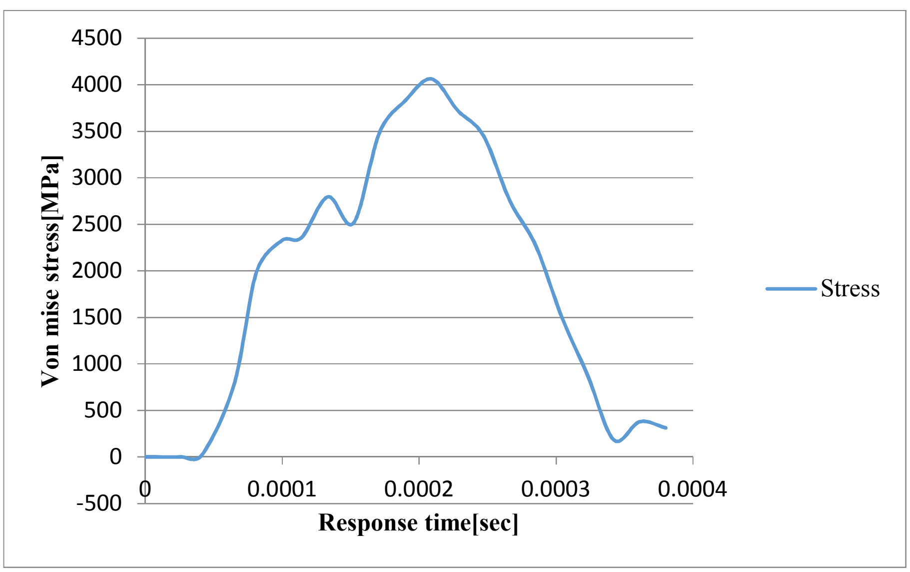

Fig.5.1.1a. Mise stress time history curve of Inverted u shaped RC shear wall at 1m standoff distance and radial direction 1

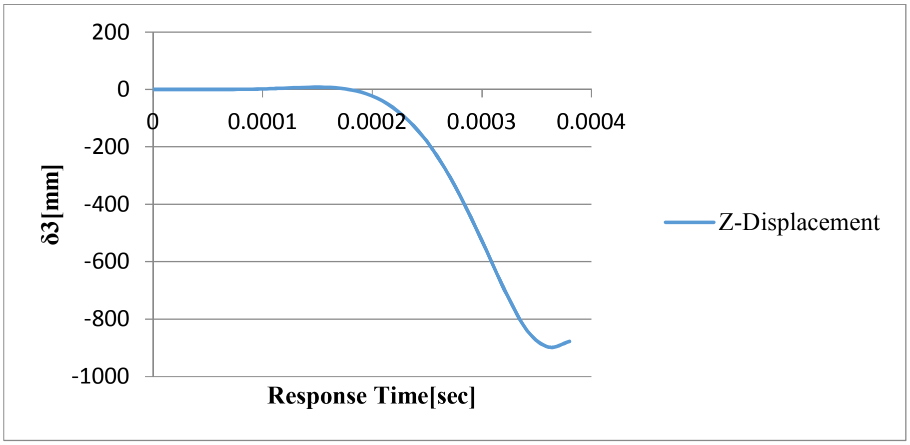

Fig.5.1.1b. Z-Displacement Time History curve of Inverted u shaped RC shear wall at 1m standoff and radial direction 1

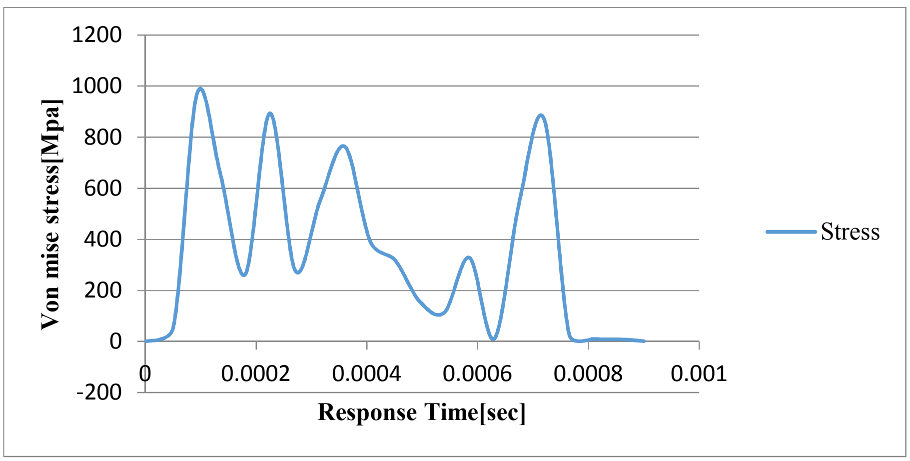

Fig.5.1.1c. Mise stresss time history curve of Inverted u shaped RC shear wall at 3m standoff and radial direction1

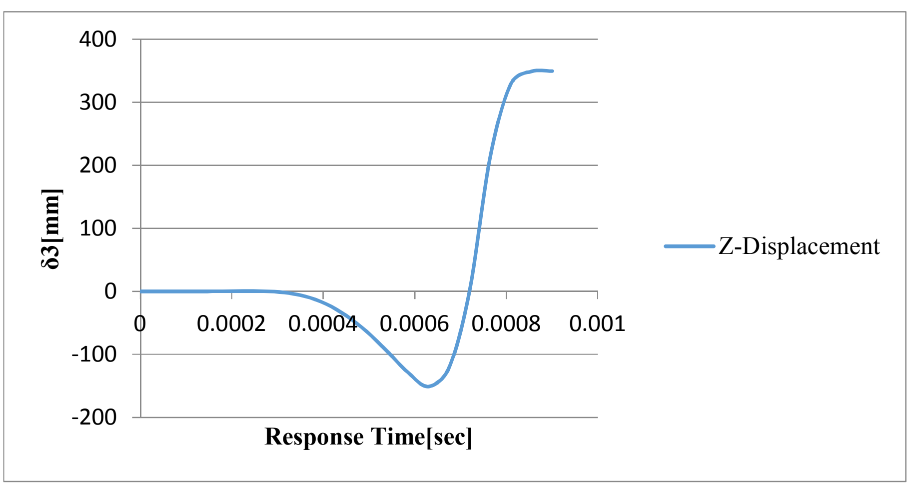

Fig.5.1.1d. Z-Displacement Time history curve of Inverted u shaped RC shear wall at 3m standoff distance and on radial direction 1

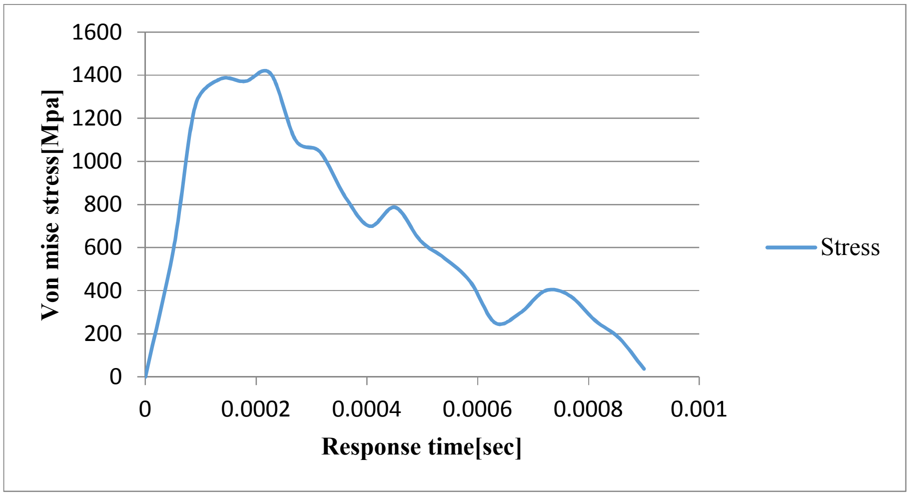

Fig.5.1.1e. Mise stress time history curve of Inverted u shaped RC shear wall at 7m standoff distance and radial direction 1

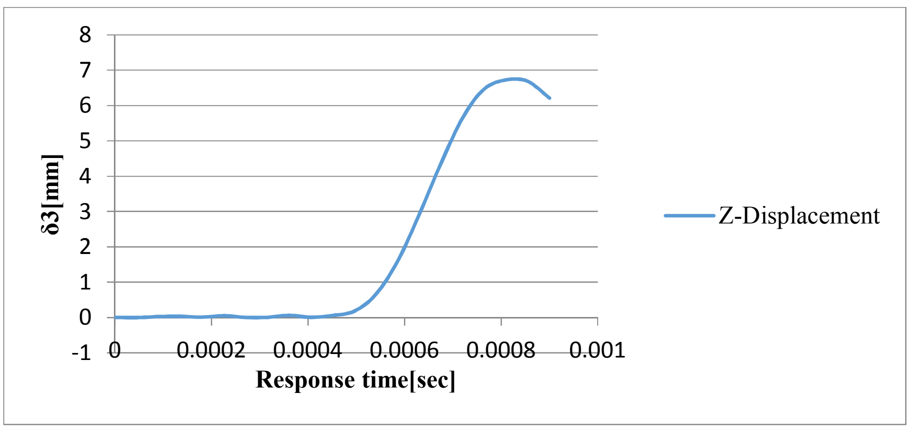

Fig.5.1.1f. Z-Displacement time history curve of Inverted u shaped RC shear wall at 7m standoff distance and radial direction 1

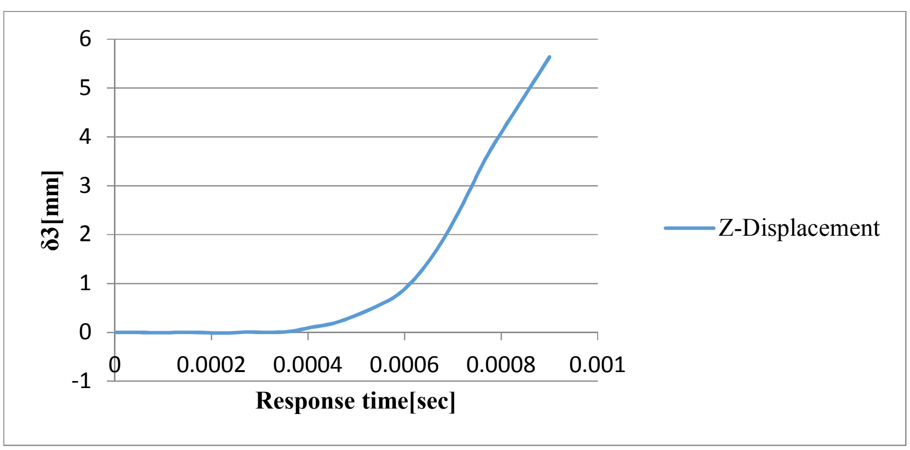

Fig.5.1.1g. Displacement time history curve of Inveretd U shaped RC shear wall at 11m and radial direction 1

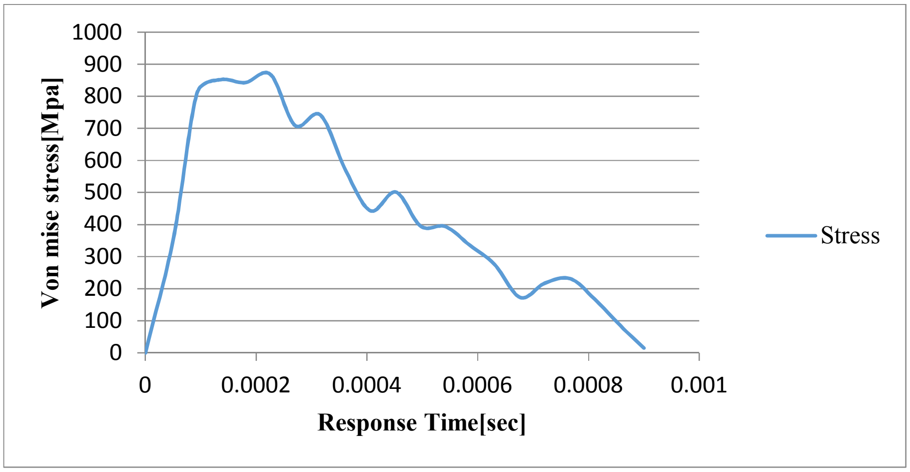

Fig.5.1.1h. Mise stress time history curve of Inverted u shaped at 11m and radial location 1

The following result graphs are show for T-section RC shear wall at 1m, 3m, 7m and 11m standoff distance from the location of RC shear wall at radial direction 1 that is in front of RC shear wall.

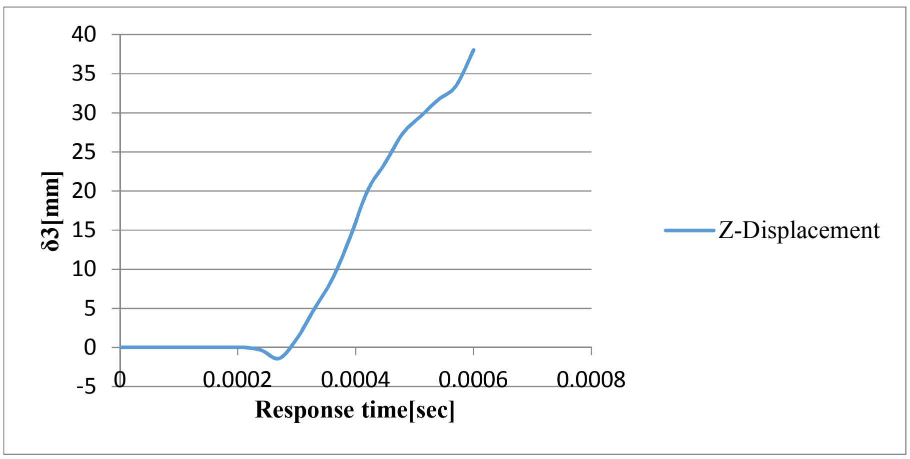

Fig.5.1.1k. Z-Displacement Time history curve of T-section at 1m standoff distance and radial direction 1

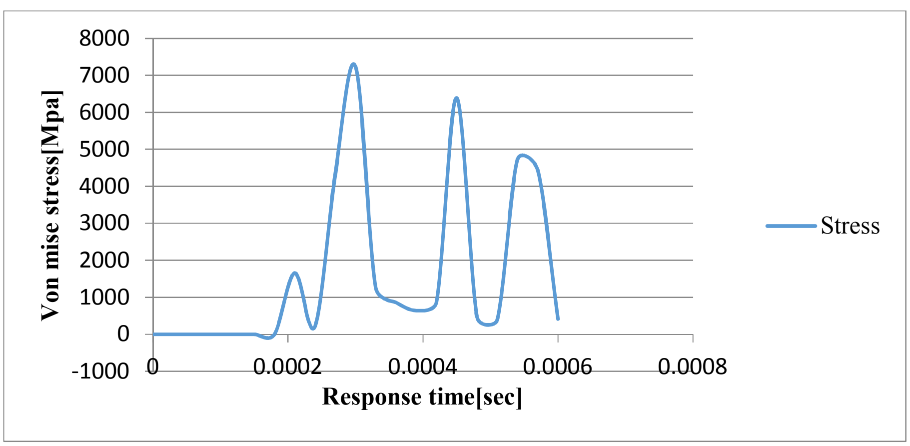

Fig.5.1.1J. Mise stress time history curve of T-section RC shear wall at 1m standoff distance and at radial direction 1

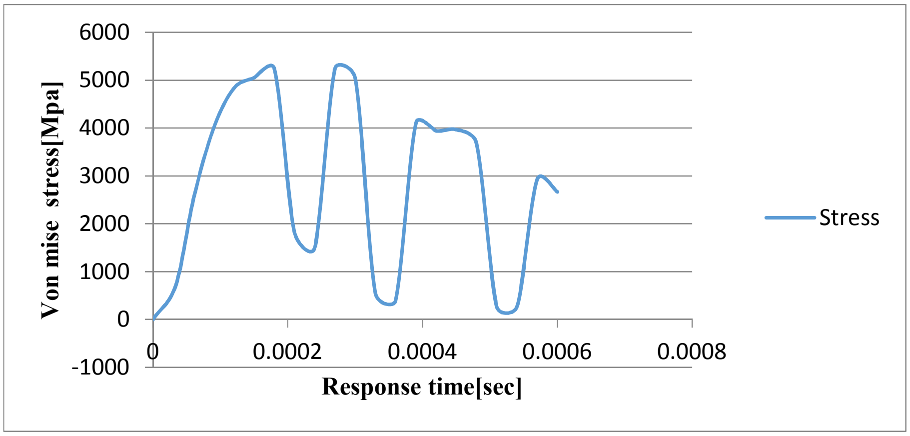

Fig.5.1.1L. Mise stress time history of T-section RC shear wall at 3m standoff distance and radial direction 1

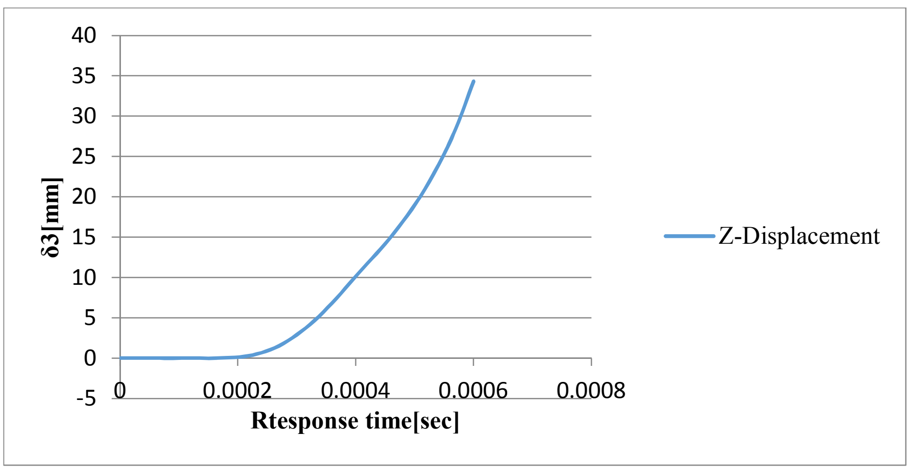

Fig.5.1.1m. Z-Displacement time history curve of T-section RC shear wall at 3m standoff distance and radial direction 1

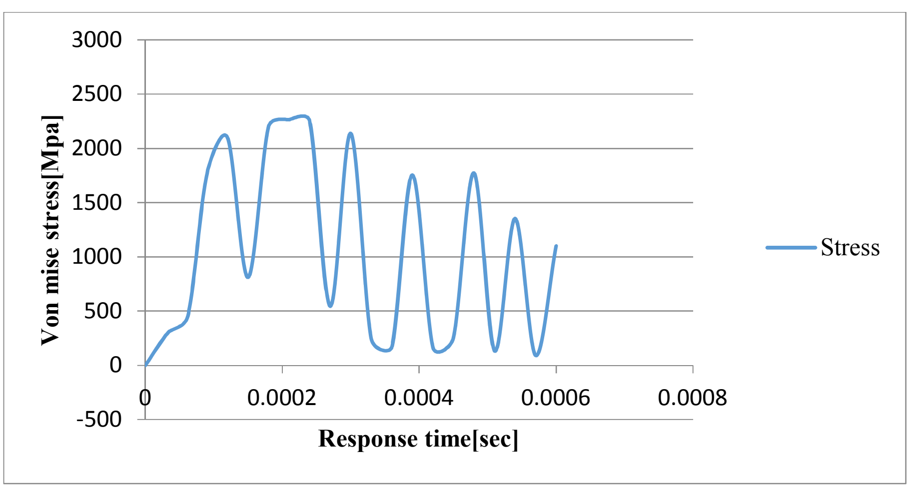

Fig. Mise stress time history curve of T-section at 7m standoff distance and radial direction 1

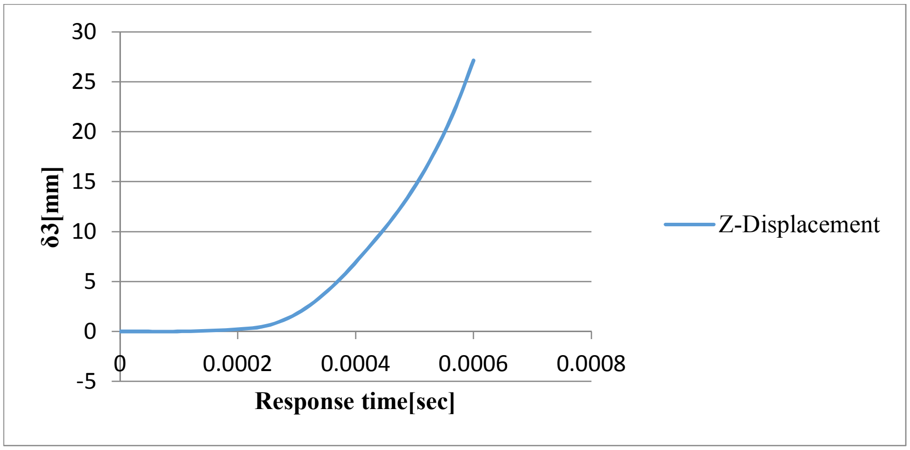

Fig.5.1.1n. Z-Displacement time history curve of T-section RC shear wall at 7m standoff distance and radial direction1

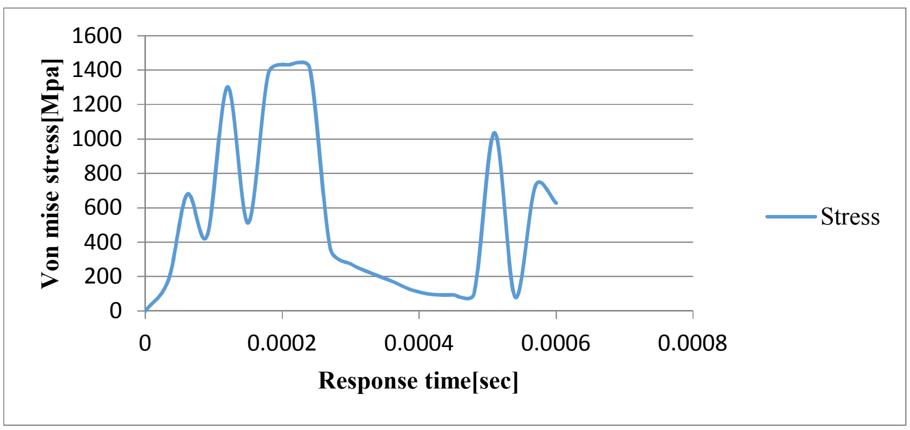

Fig.5.1.2a. Mise stress time history curve of T section RC shear wall at 11m standoff distance and radial direction 1.

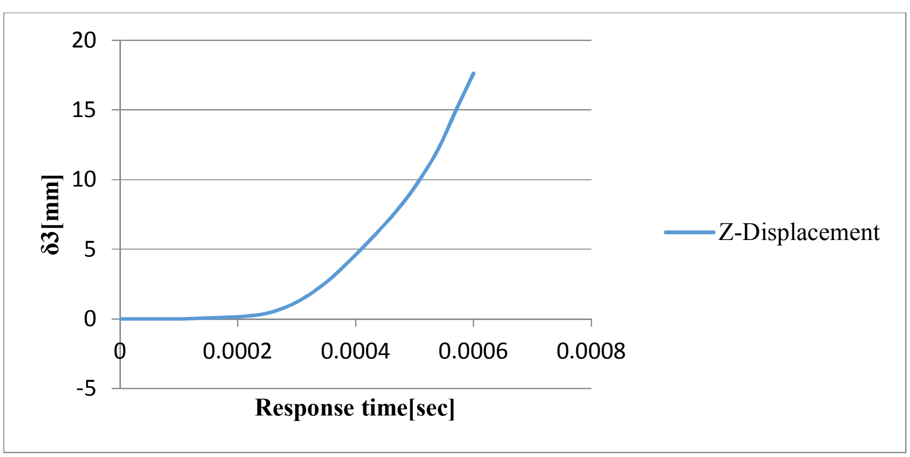

Fig.5.1.2b Z-Displacement time history curve of T-section RC shear wall at 11m standoff distance and radial direction 1

The following graphs are the result of Inverted u shaped RC shear wall and T-section RC shear wall at radial location 2 and radial location 3 at 3m standoff distance from RC shear wall.

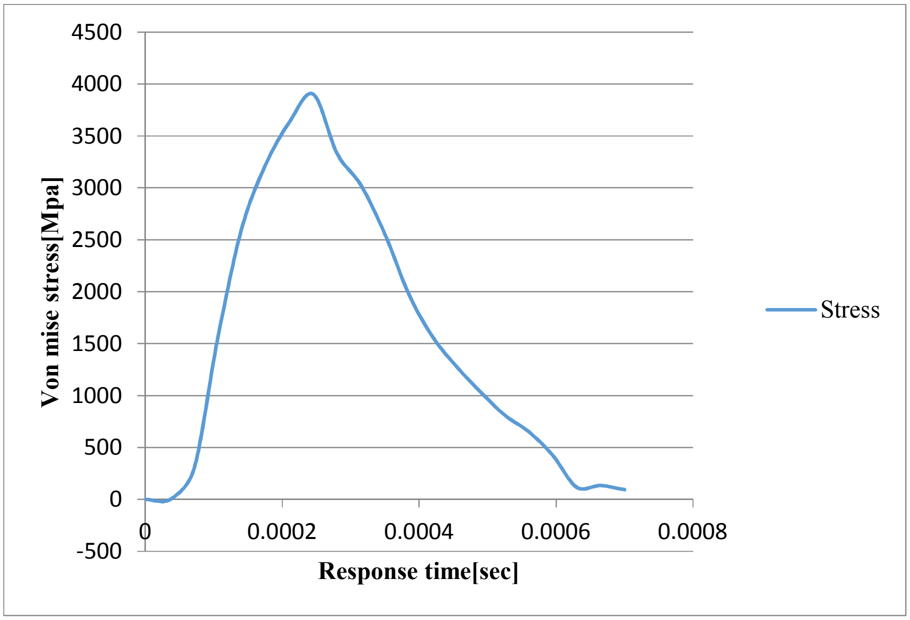

Fig.5.1.2c. Mise stress time history curve of U shaped RC shear wall at 3m standoff distance on the radial direction 2

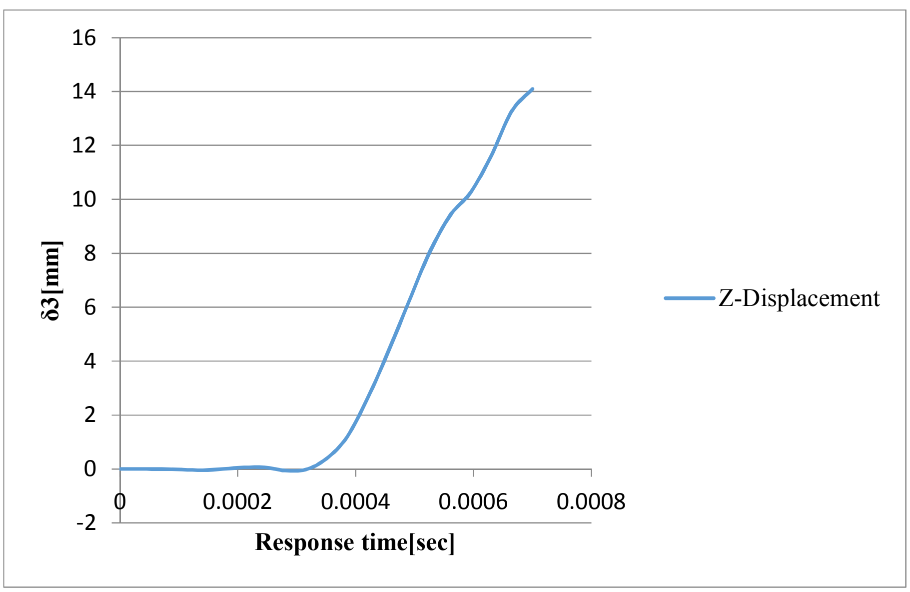

Fig.5.1.2d. Z-Displacement time history curve of inverted u shaped RC shear wall at 3m standoff distance and radial direction 2

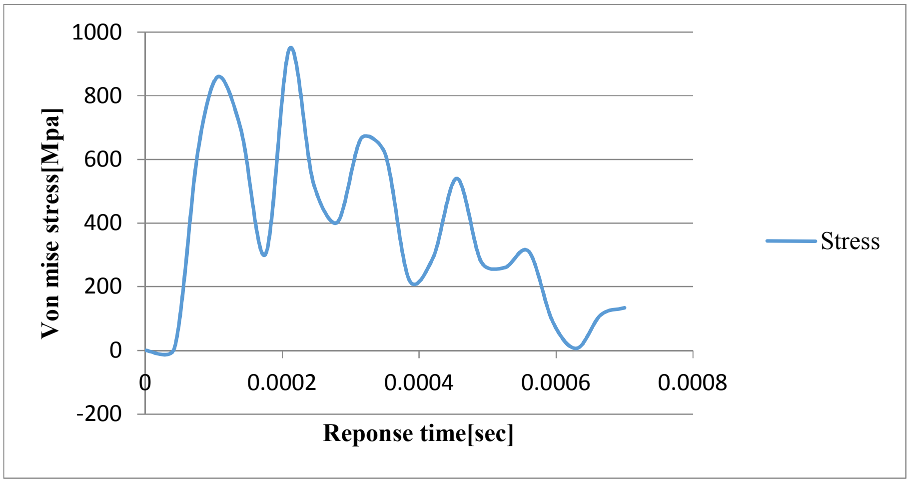

Fig.5.1.2e. Mise stress time history curve of Inverted u shaped RC shear wall at 3m standoff distance and radial direction 3

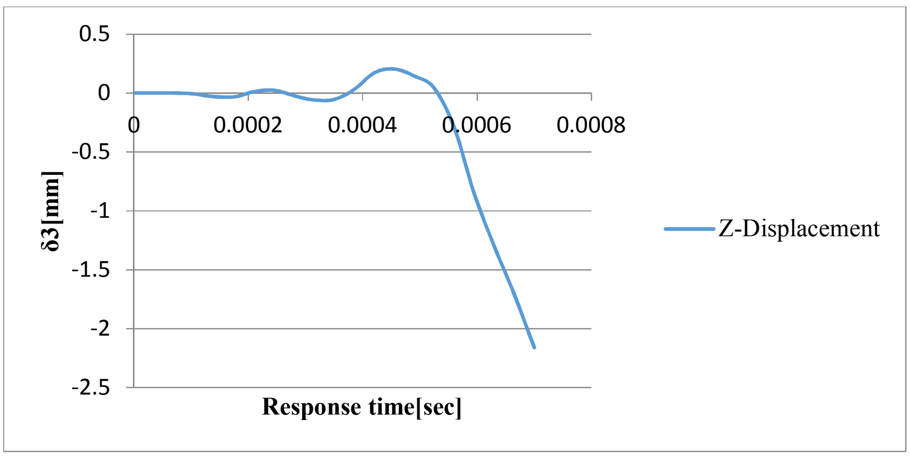

Fig.5.1.2f. Z-Displacement time history curve of Inverted u shaped RC shear wall at 3m standoff distance and radial direction 3

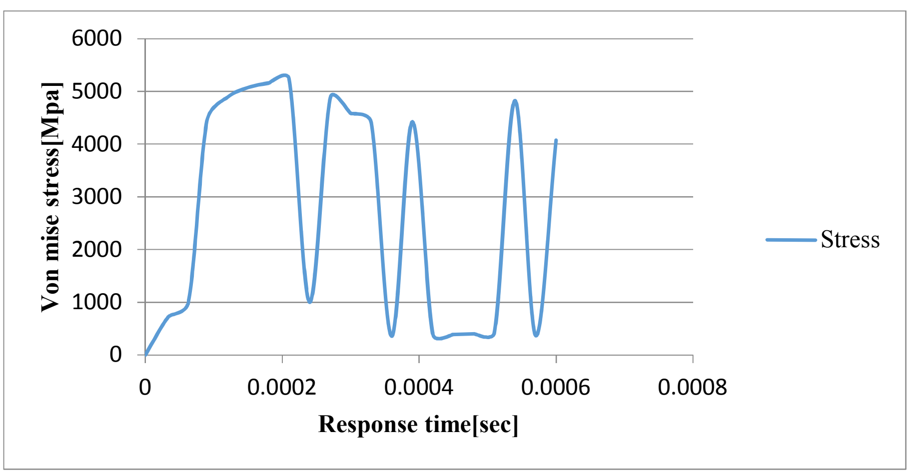

Fig.5.1.2g. Mise stress time history of T-section at 3m standoff distance and radial direction3

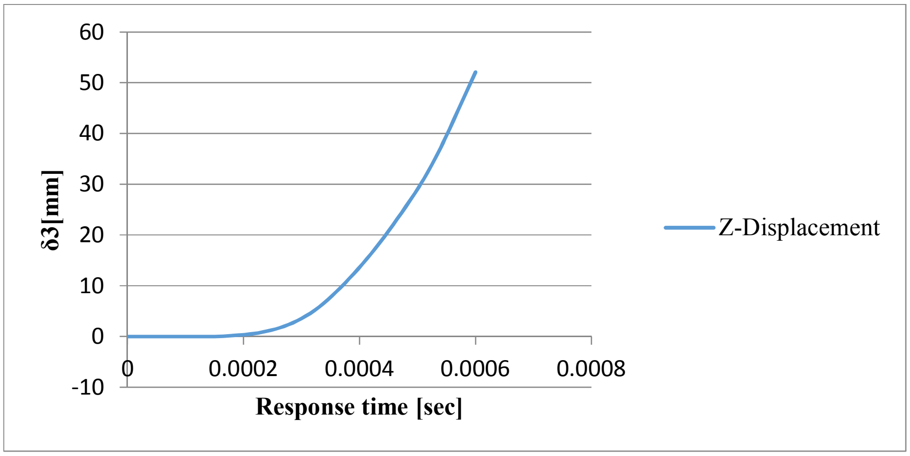

Fig.5.1.2h. Z-Displacement time history curve of T-section RC shear wall at 3m standoff distance and radial direction 3

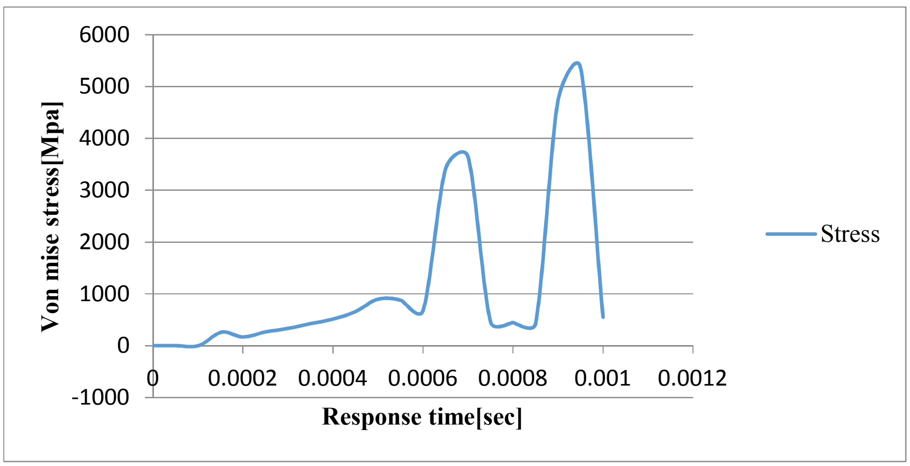

Fig.5.1.2J. Mise stress time history curve of T-section RC shear wall at 3m standoff distance and radial direction 2

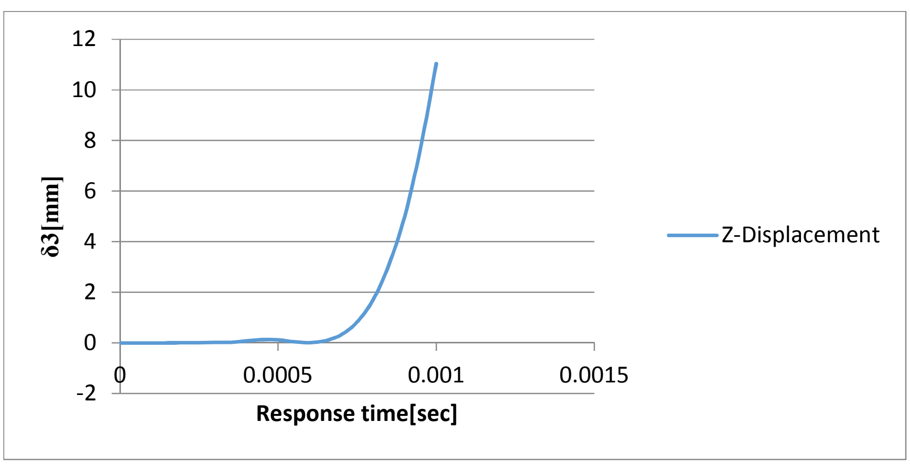

Fig.5.1.2K. Z-Displacement time history curve of T-section RC shear wall at 3m standoff distance and radial direction 2

5.2. Discussion of Results

5.2.1 Numerical Results and Comparison

As shown on above results of finite element analysis of bomb loads using ABAQUS 6.13 version numerical simulation software for different location of bomb load, at different standoff distances and different type of RC shear wall, results of peak deflection and maximum mise stress for the three types of RC shear walls at different standoff distance and at different radial direction of loading shows below. As described on chapter three of this study, the blast load radial direction1 (r1) means the load is placed in front of RC shear wall at different standoff distances, radial direction2 (r2) which has similar standoff distances from bomb load location that placed at side of T-section and inverted u-section and radial direction3 (r3) is the bomb loads are placed at different standoff distance at the rear of both T-section and Inverted RC shear wall respectively.

The deflection values and stress values with respect to Standoff distances are graphed as shows below. The following graphs shows, peak displacement response along Z direction for the three types of RC shear walls with 80mm mesh size and different standoff distance at given radial direction of loading and maximum values of mise stress for the three types of RC shear walls at different standoff distances and along similar radial load location.

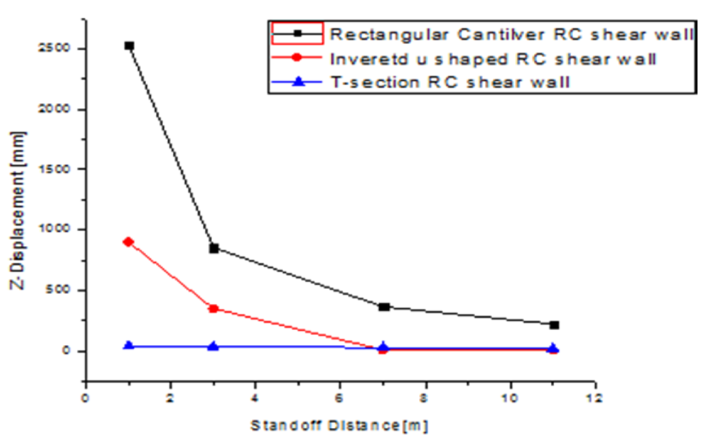

Fig.5.2a. Z-Displacement vs Standoff distance curve of rectangular RC shear wall at radial direction1 for the three RC shear wall types.

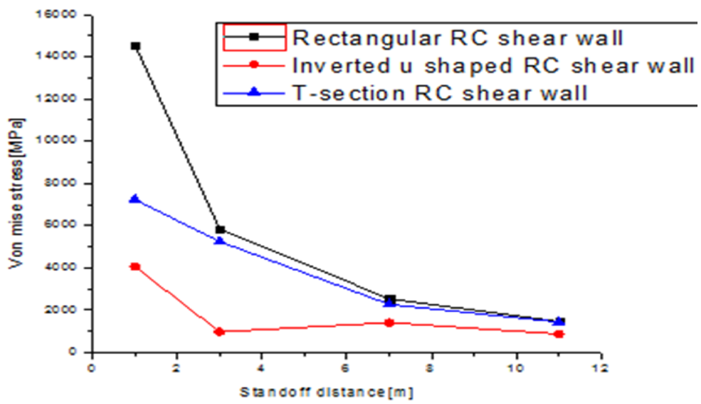

Fig.5.2b. Mise stress vs Standoff distance curve of rectangular RC shear wall at radial direction1 for the three types of RC shear walls.

X-sectional Type of RC shear wall	Standoff distance	Radial direction of loads	Mise Stress[MPa]	Z-displacement[mm]
Rectangular RC shear wall	3m	Front(r1)	5857.91	852.75
Inverted RC shear wall	3m	Front(r1)	969.911	349.911
		Side(r2)	3900.41	14.0973
		Rear(r3)	133.717	2.1608
T-section RC shear wall	3m	Front(r1)	5244.17	34.3071
		Side(r2)	5361.6	11.0374
		Rear(r3)	5235.49	52.0913

Table 5.2. Displacement and von mise stress values for different radial location of loading and at 3m standoff distance

Effect of Standoff distances

From the above Mise stress and Z-displacement graphs with respect to standoff distances such as 1m,3m,7m and 11m that also means close in case , near field cases and far field case of loading at radial load directional location 1(r1) which is the bomb placed in front of RC shear walls. From this analysis result as shown on the above comparison graphs, the maximum mise stress and maximum peak displacement along the z direction occur if the blast load placed at close in or 1m standoff distance from the location of RC shear walls. For the three types of graphs, the result of stress or displacement values for the given standoff distances, the minimum displacement and stress also occur if the bomb was placed at 11mm standoff distance for each type of RC shear wall.

Effect of radial direction of loading on response of blast

At the same standoff distance 3m that is near field, the maximum stress values if the location of load is at radial direction 1 which is in front of rectangular RC shear wall become 5857.91MPa and a maximum peak displacement value is 852.75mm from the above result table. The minimum displacement response value for Inverted u shaped RC shear wall is 2.1608mm along the z direction at radial load location 3 which is at rear side of the Inverted u shaped RC shear wall at 3m standoff distance. Similarly, the minimum peak displacement values of T-section RC shear wall is 11.0374mm at load location of radial direction of loading 2(r2) on side of T-section RC shear wall at similar 3m standoff distances. Comparison of effect of radial direction of load location as shown above result, for T-section RC shear wall peak displacement values become less if the bomb was placed at radial location of load at radial direction 3 that is on rear of RC shear wall and for Inverted u shaped RC shear wall if the bomb placed on side direction of RC shear wall. Therefore this result shows for the same standoff distance of blast, the response of displacement decrease at radial direction of load location 2 and radial location 3, for T-section and Inverted u shaped RC shear wall respectively.

Comparision of X-section on response of blast loads

To study the effect of load location, this study has three locations of loading that presented on above portion of the study and result was tabulated on the above figures and table. The tabulated result shows, for Inverted u section RC shear wall from the three types of RC shear walls, the peak deflection values are much lesser when compared peak deflection values of other sections when the bomb was placed on rear at constant 3m standoff distance and in addition to this when comparision is done for the same location of bomb for different type of x-sectional shape of RC shear walls, the inverted u shaped RC shear wall has lesser peak deflection vaue than other sections.

CHAPTER SIX

CONCLUSION AND RECOMMENDATION

6.1. Conclusion

The following conclusions can be drawn from the above numerical study presented in this paper.

When a stand- off distance was 1m and the weight of bomb was 5kg, the pressure loads became 155.53Pa and the stand -off distance equaled to 11 m and a weight of bomb was 5kg, the pressure blast load was 13.62pa. From this and above shown result conclude that the standoff distance increased, the pressure distribution decreased.

Generally for blast load analysis, distance from blast load (bomb) to target (RC shear wall) is one of critical variable. It implies that standoff distance affect the magnitude of pressure distribution and effect on target.

The location of blast in front of RC shear walls, there was high displacement response value than other two radial locations of loading. Peak minimum displacement and peak minimum stress response occur if the blast was placed at side of T-section and rear of Inverted u shaped RC shear walls. Therefore, for the same standoff distance, radial load location of bomb has impact on blast resistance of RC shear wall.

Inverted U-shape RC shear wall, for the same type of load from the above results, when the bomb is placed rear, the value of stress and displacement values are lower than similar bomb load that placed on side and front of RC shear wall. Therefore the location has an impact on the result of bomb load analysis.

Similarly when compared the three x-section of RC shear wall result shows, for the same type of loads and the same standoff distance 3m from RC shear wall, displacement became decrease from 2.1608mm of Inverted u shaped RC shear wall value to a value of 52.0913mm of displacement for T-section RC shear wall. Therefore displacement decreases for Inverted u-section. It is possible to conclude, The Inverted u section is more effective on response of bomb. This means from the three RC shear walls, the more effective type of RC shear wall in blast resistance is Inverted u shaped RC shear wall.

6.2. Recommendation

All the above analysis and result shows that it is a must to consider the blast loads like bomb on any type of structure for future analysis and design of structures. Because it's affect the life of peoples and structural failure or damage.

For reinforced concrete structure in future work it is necessary to use different thicness of RC shear wall and different reinforcement bar ratios to study the effect of reinforcement ratios and thickness of RC shear wall for blast response.

The response analysis of building which have RC shear wall on finite element method will be a future work.

References

[1] Agrawal , A. K., and Yi, Z. (2009). TRB Rep., High prediction Analysis of Blast Events on Highway Bridges, City College of New York, New York.

[2] Biggs, J.M, Introduction to Structural Dynamics, McGraw-Hill, New York, 1964.

[3] Brode , H.L.,"Numerical Solution of Spherical blast Waves" , Journal of Applied Physics ,American Institute of Physics ,New York, 1955.

[4] Ngo. D. Schordelis and A.C.,(1967), "Finite Element Analysis of Reinforced Concrete Beams",Journal of ACI report, 153-163.

[5] Barmejo M. Gabaldon F.S.A and Goicolea (2011), "Impact and explosive loads on concrete buildings using shell and beam type elements", ECOMAS Thematic conference on computational methods in structural dynamics and earthquake engineering , Greece.

[6] Agrawal, A. K., Alampalli, S., and Ettouney, M. (2009).,"Stakeholders Perspective on multi hazards and natural hazards." ,2009 workshop on Aging Infrastructure, The DHS Science and Technology Directorate Washington, DC, 82-86.

[7] ABAQUS user manual, 2008.

[8] Ronald, L.S. ," Response of wide flange steel columns subjected to constant axial load and lateral blast load",civil engineering Department,Virginia , Blacksburg , 2006.

[9] Ngo.T.,Mendis .P., Gupta .P. , Ramsay .J. ,"Blast Loading and blast effects on structure ",the University of melbourne, australia ,2007.

[10] Hibbit, H.D. (1984),"A general purpose finite element code with emphasis on nonlinear applications" ,Journal of Nuclear Engineering and design , 77:3.

[11]Gunjan S., Kavya T. and Ganesh T. (2005) , " Finite Element Analysis and Experimental Validation of RC Single mat slabs subjected to blast loads." , department of civil engineering , University of Missouri Kanas , 352 Flarsheim hall ,5100 Rock hill Road, Kanas city ,MO-64110.

[12] Kamali Abbas Zangeneh , (2012), " shear strength of reinforced concerete beams subjected to blast loading", Stockhol.

[13] Fischinger M. Vidic T. Selih J. Fajafar P. Zhang .H.Y. and Damjanic F.B. (1990) , "Validation of a macroscopic model for cyclic response prediction of RC walls."

[14]. Kim D.A, and Foutch, T. "A simplified model strategy for R/C walls", Jucturesournal of Engineering structure, 2007.1197-1208

[15]. Kim, D.A and Foutch, T. , 2007, "Applications of FEMA methodology to RC shear wall buildings governed by flexure", journal of engineering structures, 29:10.

APPENDIX

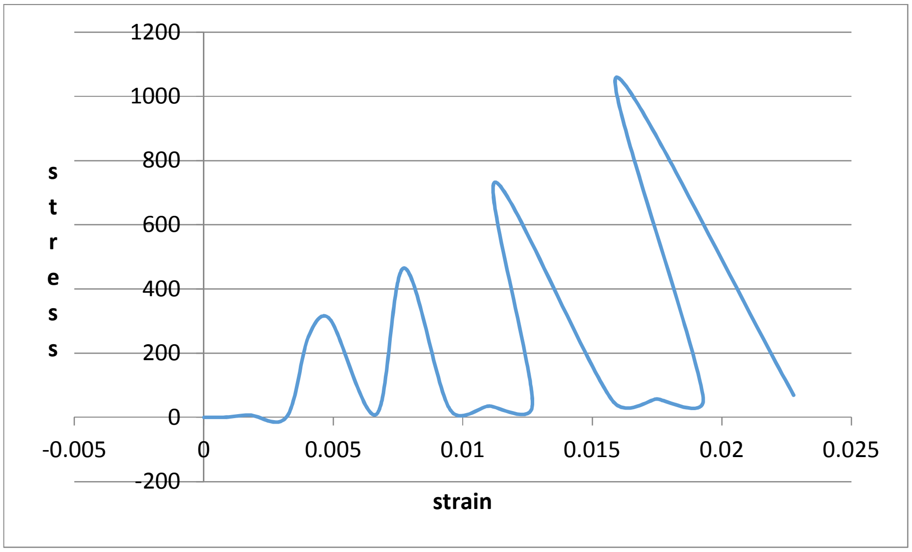

Fig.8.1a. Stress strain of cantilever RC shear wall with 25,4mm mesh and 0.0346% reinforcement ratio

Maximum stress from stress time curve and stress strain values are 3224.56MPa and 1059.52MPa respectively.

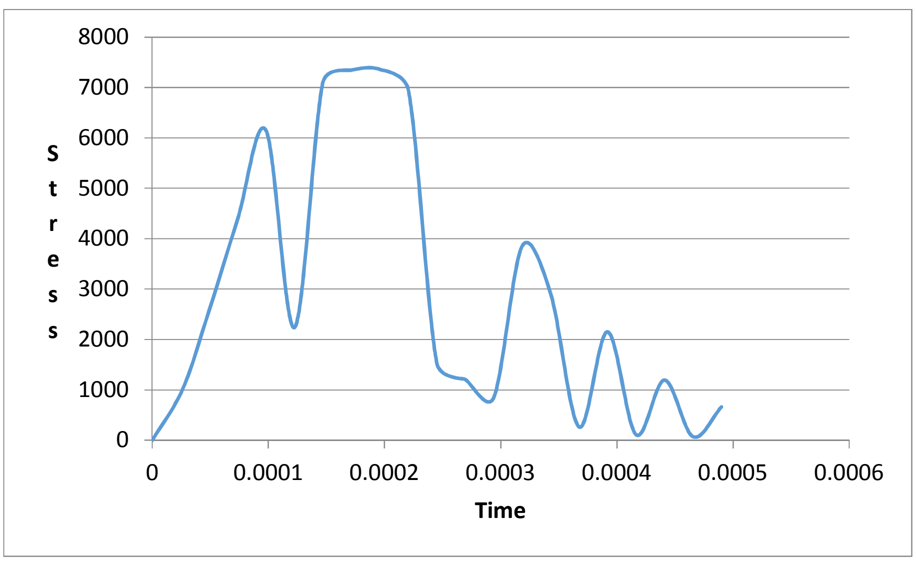

Fig. 8.2b.Stress time history of 0.018% reinforcement ratio and 25.4mm mesh

```
********************************************************************************
Field Output Report, written Tue Nov 01 11:19:57 2016

Source 1
---------

   ODB: C:/Users/him/ABAQUS Temp file/u-blast-1.odb
   Step: blast load
   Frame: Increment       166: Step Time =   6.0083E-04

Loc 1 : Nodal values from source 1

Output sorted by column "Node Label".

Field Output reported at nodes for part: horizontal bar 1-1

            Node     A.Magnitude
           Label          @Loc 1
---------------------------------
               1         3.75599
               2     31.7920E+06
               3         6.12715
               4     37.4854E+06
               5         6.78674
               6     39.9112E+06
               7         6.32848
               8     37.8247E+06
               9         6.41863
              10     21.9225E+06
              11         6.92136
              12     25.6361E+06
              13         6.34125
              14     31.1661E+06
              15         6.53962
              16     39.8724E+06
              17         6.38318
              18     39.7933E+06
              19         5.61828
              20     34.7391E+06
              21     535.806E-03
              22     5.30226E+06
              23         36.3422
              24         105.740
              25         736.481
              26     2.44989E+03
              27     11.6297E+03
              28     36.7753E+03
              29     124.009E+03
              30     340.451E+03
              31     854.526E+03
              32     1.95026E+06
              33     3.94263E+06
              34     6.55144E+06
              35     7.79007E+06
              36     7.72006E+06
              37     12.0153E+06
```

38	23.9315E+06
39	29.9715E+06
40	30.4987E+06
41	55.8791
42	169.307
43	1.13203E+03
44	3.84332E+03
45	17.7787E+03
46	56.5510E+03
47	186.806E+03
48	510.452E+03
49	1.25776E+06
50	2.83367E+06
51	5.67785E+06
52	9.02954E+06
53	9.66942E+06
54	8.66675E+06
55	15.2306E+06
56	29.5012E+06
57	35.7405E+06
58	35.1297E+06
59	58.6324
60	181.988
61	1.18744E+03
62	4.06410E+03
63	18.5775E+03
64	59.2127E+03
65	194.729E+03
66	532.086E+03
67	1.31185E+06
68	2.95008E+06
69	5.89483E+06
70	9.36253E+06
71	10.1703E+06
72	9.43003E+06
73	16.2297E+06
74	31.0890E+06
75	38.1530E+06
76	37.9992E+06
77	56.9690
78	173.999
79	1.15515E+03
80	3.93577E+03
81	18.1453E+03
82	57.7873E+03
83	190.658E+03
84	521.110E+03
85	1.28416E+06
86	2.89116E+06
87	5.78930E+06
88	9.21814E+06

The displacement value of inverted U shaped RC shear wall for some nodes

```
********************************************************************************
Field Output Report, written Tue Nov 01 11:27:19 2016

Source 1
---------

   ODB: C:/Users/him/ABAQUS Temp file/u-blast-1.odb
   Step: blast load
   Frame: Increment       166: Step Time =   6.0083E-04

Loc 1 : Nodal values from source 1

Output sorted by column "Node Label".

Field Output reported at nodes for part: horizontal bar 1-1

            Node     U.Magnitude
           Label          @Loc 1
---------------------------------
               1     329.476E-12
               2     424.474E-03
               3     535.575E-12
               4     550.386E-03
               5     603.475E-12
               6     560.195E-03
               7     553.212E-12
               8     554.397E-03
               9     579.833E-12
              10     493.164E-03
              11     643.045E-12
              12     510.074E-03
              13     559.275E-12
              14     537.931E-03
              15     575.694E-12
              16     558.659E-03
              17     558.951E-12
              18     557.723E-03
              19     496.644E-12
              20     519.607E-03
              21     45.8731E-12
              22     77.9519E-03
              23     4.55953E-09
              24     12.1513E-09
              25     114.864E-09
              26     373.504E-09
              27     2.35094E-06
              28     7.80146E-06
              29     34.8494E-06
              30     109.861E-06
              31     381.769E-06
              32     1.09940E-03
              33     3.13260E-03
              34     8.18902E-03
              35     19.4182E-03
              36     42.0755E-03
              37     87.3235E-03
```

```
 38      175.121E-03
 39      293.151E-03
 40      377.209E-03
 41      6.93700E-09
 42      19.3532E-09
 43      174.429E-09
 44      583.348E-09
 45      3.55584E-06
 46      11.9489E-06
 47      52.1948E-06
 48      164.790E-06
 49      561.993E-06
 50      1.60765E-03
 51      4.53570E-03
 52      11.6865E-03
 53      27.2068E-03
 54      57.1066E-03
 55      116.502E-03
 56      231.897E-03
 57      384.248E-03
 58      490.795E-03
 59      7.27634E-09
 60      21.0193E-09
 61      182.901E-09
 62      620.909E-09
 63      3.71350E-06
 64      12.5637E-06
 65      54.3668E-06
 66      172.112E-06
 67      584.164E-06
 68      1.67172E-03
 69      4.69830E-03
 70      12.0440E-03
 71      27.8635E-03
 72      58.1515E-03
 73      118.101E-03
 74      234.930E-03
 75      391.057E-03
 76      498.614E-03
 77      7.05469E-09
 78      19.8729E-09
 79      177.497E-09
 80      596.665E-09
 81      3.61864E-06
 82      12.1871E-06
 83      53.0915E-06
 84      167.722E-06
 85      571.082E-06
 86      1.63240E-03
 87      4.59986E-03
 88      11.8367E-03
```

```
Displacement values of RC shear wall with 80mm mesh size

*****************************************************************
*********
```

```
Field Output Report, written Tue Nov 01 11:33:06 2016

Source 1
---------

   ODB: C:/Users/him/ABAQUS Temp file/blast.odb
   Step: blast
   Frame: Increment      6005: Step Time =   2.9401E-04

Loc 1 : Nodal values from source 1

Output sorted by column "Node Label".

Field Output reported at nodes for part: horizontal re-bar-1

            Node     U.Magnitude
           Label           @Loc 1
---------------------------------
               1        9.76113
               2        9.76406
               3        14.4116
               4        14.4133
               5        14.0768
               6        14.0736
               7        14.0510
               8        14.0516
               9        14.0472
              10        14.0474
              11        14.0551
              12        14.0552
              13        14.0453
              14        14.0451
              15        14.0561
              16        14.0559
              17        14.0583
              18        14.0579
              19        13.9602
              20        13.9604
              21        13.3448
              22        13.3453
              23        14.0493
              24        14.0492
              25        14.0608
              26        14.0606
              27        14.0519
              28        14.0517
              29        14.0527
              30        14.0530
              31        14.0528
              32        14.0528
              33        14.0445
              34        14.0447
              35        14.0576
              36        14.0581
              37        14.1301
              38        14.1218
              39        14.0077
```

40	13.9899
41	14.0475
42	14.0476
43	9.75403
44	9.75102
45	9.74760
46	9.74608
47	9.74738
48	9.75149
49	9.75760
50	9.76534
51	9.77419
52	9.78318
53	9.79172
54	9.80523
55	9.82800
56	9.85163
57	9.87389
58	9.89472
59	9.91406
60	9.93197
61	9.94851
62	9.96379
63	9.97772
64	9.99020
65	10.0011
66	10.0168
67	10.0399
68	10.0616
69	10.0820
70	10.1010
71	10.1184
72	10.1346
73	10.1489
74	10.1614
75	10.1722
76	10.1811
77	10.1888
78	10.2008
79	10.2178
80	10.2326
81	10.2448
82	10.2549
83	10.2627
84	10.2684
85	10.2718
86	10.2733
87	10.2733
88	10.2716

Acceleration and reaction force results of RC cantilever shear wall with 80mm mesh sizes

```
********************************************************************************
Field Output Report, written Tue Nov 01 11:37:00 2016

Source 1
---------

   ODB: C:/Users/him/ABAQUS Temp file/blast.odb
   Step: blast
   Frame: Increment      6005: Step Time =   2.9401E-04

Loc 1 : Nodal values from source 1

Output sorted by column "Node Label".

Field Output reported at nodes for part: horizontal re-bar-1

            Node     A.Magnitude    RF.Magnitude
           Label          @Loc 1          @Loc 1
-------------------------------------------------
               1     264.921E+06              0.
               2     104.998E+06              0.
               3     3.08490E+09              0.
               4     3.42610E+09              0.
               5     3.27077E+09              0.
               6     3.26318E+09              0.
               7     3.06028E+09              0.
               8     3.03259E+09              0.
               9     3.12468E+09              0.
              10     3.14326E+09              0.
              11     3.34075E+09              0.
              12     3.35846E+09              0.
              13     3.05199E+09              0.
              14     3.03589E+09              0.
              15     3.26853E+09              0.
              16     3.28013E+09              0.
              17     3.25731E+09              0.
              18     3.26280E+09              0.
              19     3.26667E+09              0.
              20     3.19852E+09              0.
              21     3.17108E+09              0.
              22     3.25736E+09              0.
              23     3.00580E+09              0.
              24     3.01214E+09              0.
              25     3.24162E+09              0.
              26     3.25512E+09              0.
              27     3.02428E+09              0.
              28     3.05761E+09              0.
              29     3.34078E+09              0.
              30     3.35046E+09              0.
              31     3.34478E+09              0.
              32     3.34300E+09              0.
              33     3.04459E+09              0.
              34     3.07437E+09              0.
              35     3.31905E+09              0.
              36     3.31952E+09              0.
              37     3.20467E+09              0.
```

38	3.39899E+09	0.
39	2.66077E+09	0.
40	2.45619E+09	0.
41	3.15357E+09	0.
42	3.13070E+09	0.
43	2.34760E+09	0.
44	2.73565E+09	0.
45	2.13882E+09	0.
46	2.57622E+09	0.
47	3.11757E+09	0.
48	3.65589E+09	0.
49	4.31766E+09	0.
50	3.23241E+09	0.
51	484.411E+06	0.
52	1.19875E+09	0.
53	2.90201E+09	0.
54	3.37732E+09	0.
55	2.53015E+09	0.
56	1.47561E+09	0.
57	1.70434E+09	0.
58	1.47481E+09	0.
59	1.88565E+09	0.
60	2.98430E+09	0.
61	1.64773E+09	0.
62	1.61087E+09	0.
63	1.18424E+09	0.
64	1.15828E+09	0.
65	2.24630E+09	0.
66	2.45531E+09	0.
67	3.27006E+09	0.
68	2.14692E+09	0.
69	1.41086E+09	0.
70	1.49283E+09	0.
71	1.43288E+09	0.
72	1.26618E+09	0.
73	1.03845E+09	0.
74	1.38008E+09	0.
75	1.17630E+09	0.
76	1.60521E+09	0.
77	2.08529E+09	0.
78	2.28284E+09	0.
79	2.20703E+09	0.
80	2.65934E+09	0.
81	1.21916E+09	0.
82	3.48463E+09	0.
83	2.46881E+09	0.
84	2.49598E+09	0.
85	1.20321E+09	0.
86	1.75610E+09	0.
87	4.21869E+09	0.
88	3.05494E+09	0.

The maximum principal strain values of cantilever RC shear wall for some nodes

```
*********************************************************************************
Field Output Report, written Tue Nov 01 11:41:32 2016

Source 1
---------

   ODB: C:/Users/him/ABAQUS Temp file/blast.odb
   Step: blast
   Frame: Increment      6005: Step Time =   2.9401E-04

Loc 1 : Nodal values from source 1

Output sorted by column "Node Label".

Field Output reported at nodes for part: horizontal re-bar-1
   Computation algorithm: EXTRAPOLATE_COMPUTE_AVERAGE
   Averaged at nodes
   Averaging regions: ODB_REGIONS

           Node     PE.Max. Prin
          Label           @Loc 1
---------------------------------
              1     16.4829E-03
              2     16.4658E-03
              3     60.9902E-03
              4     61.1529E-03
              5     70.1337E-03
              6     70.5217E-03
              7     70.5764E-03
              8     70.5626E-03
              9     70.5314E-03
             10     70.5200E-03
             11     70.5861E-03
             12     70.5882E-03
             13     70.5033E-03
             14     70.5007E-03
             15     70.4797E-03
             16     70.4840E-03
             17     70.1717E-03
             18     70.1684E-03
             19     69.0944E-03
             20     69.0961E-03
             21     67.4005E-03
             22     67.4113E-03
             23     69.9268E-03
             24     69.9219E-03
             25     70.2611E-03
             26     70.2656E-03
             27     70.5525E-03
             28     70.5580E-03
             29     70.5600E-03
             30     70.5653E-03
             31     70.5588E-03
             32     70.5592E-03
             33     70.5111E-03
```

34	70.4985E-03
35	70.5317E-03
36	70.5646E-03
37	68.3362E-03
38	68.9993E-03
39	46.4086E-03
40	46.5444E-03
41	70.5269E-03
42	70.5295E-03
43	16.0416E-03
44	15.1618E-03
45	14.2578E-03
46	13.2785E-03
47	12.2067E-03
48	11.0817E-03
49	9.92587E-03
50	8.76498E-03
51	7.64421E-03
52	6.56751E-03
53	5.51596E-03
54	4.52725E-03
55	3.67910E-03
56	2.94406E-03
57	2.28070E-03
58	1.68622E-03
59	1.15830E-03
60	708.619E-06
61	328.259E-06
62	76.3040E-06
63	0.
64	0.
65	0.
66	0.
67	0.
68	0.
69	0.
70	0.
71	0.
72	0.
73	0.
74	0.
75	0.
76	0.
77	0.
78	0.
79	0.
80	0.
81	0.
82	0.
83	0.
84	0.
85	0.
86	0.
87	0.
88	0.
89	0.
90	0.

91	0.
92	0.
93	0.
94	0.
95	0.
96	0.
97	0.
98	0.
99	0.
100	0.
101	0.
102	0.
103	0.
104	0.
105	0.
106	0.
107	0.
108	0.
109	0.
110	0.
111	0.
112	0.
113	0.
114	0.
115	0.
116	0.
117	0.
118	0.
119	0.
120	0.
121	0.
122	0.
123	0.
124	0.
125	0.
126	0.
127	0.
128	0.
129	0.
130	0.
131	0.
132	0.
133	0.
134	0.
135	0.
136	0.
137	0.
138	0.
139	0.

```
The following values are reaction forces, special displacements and
plastic strain values for T-section RC shear wall section for some
nodes

**********************************************************************
*********
Field Output Report, written Tue Nov 01 11:47:09 2016

Source 1
---------

   ODB: C:/Users/him/ABAQUS Temp file/tjob-1.odb
   Step: blast
   Frame: Increment     66200: Step Time =   1.0000E-03

Loc 1 : Nodal values from source 1

Output sorted by column "Node Label".

Field Output reported at nodes for part: concrete t-section-1
   Computation algorithm: EXTRAPOLATE_COMPUTE_AVERAGE
   Averaged at nodes
   Averaging regions: ODB_REGIONS

           Node     RF.Magnitude      U.Magnitude    PE.Max. Prin
          Label           @Loc 1           @Loc 1          @Loc 1
-----------------------------------------------------------------
              1      1.44060E+09               0.         1.34670
              2      8.00707E+09               0.         1.23224
              3      3.90094E+09               0.         1.25148
              4      1.47773E+09               0.         1.19493
              5      7.88554E+09               0.         1.29540
              6      279.182E+06               0.         1.17740
              7      233.726E+06               0.         1.17615
              8      3.19976E+09               0.         1.38096
              9      1.98522E+09               0.         1.11218
             10      2.16779E+09               0.         1.10405
             11      6.37413E+09               0.         1.28134
             12      14.5562E+09               0.         1.14086
             13      12.0993E+09               0.         1.01551
             14      11.7903E+09               0.     920.634E-03
             15      6.69933E+09               0.         1.00098
             16      9.80923E+09               0.         1.11167
             17      11.7429E+09               0.     983.590E-03
             18      10.8884E+09               0.         1.01181
             19      9.21183E+09               0.     995.040E-03
             20      11.1732E+09               0.     868.625E-03
             21      10.9201E+09               0.         1.00770
             22      6.35487E+09               0.         1.23064
             23      8.14039E+09               0.         1.15414
             24      9.64671E+09               0.     836.940E-03
             25      12.6395E+09               0.     801.742E-03
             26      11.2982E+09               0.     865.718E-03
             27      10.1366E+09               0.     834.791E-03
             28      11.0638E+09               0.     854.517E-03
             29      7.90021E+09               0.     784.439E-03
             30      5.37213E+09               0.     807.386E-03
```

31	7.55028E+09	0.	928.210E-03
32	10.6985E+09	0.	797.004E-03
33	7.94874E+09	0.	680.908E-03
34	4.53144E+09	0.	647.823E-03
35	6.23565E+09	0.	590.114E-03
36	8.40574E+09	0.	567.776E-03
37	9.99828E+09	0.	676.742E-03
38	12.5997E+09	0.	780.388E-03
39	14.0922E+09	0.	660.156E-03
40	16.0871E+09	0.	584.291E-03
41	14.1036E+09	0.	591.864E-03
42	9.00812E+09	0.	589.370E-03
43	18.0894E+09	0.	614.317E-03
44	18.6589E+09	0.	608.820E-03
45	17.3004E+09	0.	767.544E-03
46	9.12557E+09	0.	1.02431
47	5.97952E+09	0.	1.10991
48	13.5249E+09	0.	1.12949
49	15.3640E+09	0.	1.12192
50	18.2004E+09	0.	1.07136
51	17.5499E+09	0.	952.636E-03
52	11.3442E+09	0.	1.06468
53	1.94026E+09	0.	916.773E-03
54	3.20470E+09	0.	888.498E-03
55	4.26272E+09	0.	1.15705
56	3.17338E+09	0.	1.13121
57	2.63336E+09	0.	1.15440
58	3.49615E+09	0.	1.22652
59	2.69156E+09	0.	1.25760
60	4.41564E+09	0.	1.15502
61	3.77473E+09	0.	1.06230
62	1.78036E+09	0.	993.024E-03
63	1.66192E+09	0.	990.864E-03
64	4.70978E+09	0.	968.047E-03
65	2.41926E+09	0.	947.356E-03
66	5.42388E+09	0.	1.05605
67	4.08075E+09	0.	1.03871
68	3.67537E+09	0.	847.794E-03
69	4.87053E+09	0.	692.347E-03
70	3.90930E+09	0.	627.354E-03
71	1.14863E+09	0.	592.730E-03
72	2.19097E+09	0.	596.783E-03
73	5.29556E+09	0.	688.346E-03
74	420.492E+06	0.	1.38851
75	424.180E+06	0.	718.577E-03
76	307.280E+06	0.	714.107E-03
77	186.315E+06	0.	721.706E-03
78	193.045E+06	0.	756.879E-03
79	417.500E+06	0.	806.047E-03
80	317.751E+06	0.	812.733E-03
81	431.124E+06	0.	809.325E-03
82	307.608E+06	0.	871.992E-03
83	539.846E+06	0.	904.078E-03
84	495.790E+06	0.	901.753E-03
85	86.4470E+06	0.	971.007E-03
86	467.736E+06	0.	1.00189
87	248.550E+06	0.	1.03413

88	364.133E+06	0.	1.10078
89	424.009E+06	0.	1.13797
90	179.779E+06	0.	1.13187
91	376.229E+06	0.	1.14778
92	547.329E+06	0.	1.18592
93	232.012E+06	0.	1.17763
94	456.546E+06	0.	1.17700
95	469.762E+06	0.	1.17307
96	997.136E+06	0.	1.13560
97	101.553E+06	0.	1.08614
98	379.082E+06	0.	1.05625
99	205.919E+06	0.	1.07648
100	342.980E+06	0.	1.04475
101	328.998E+06	0.	1.00327
102	236.851E+06	0.	1.01127
103	332.177E+06	0.	977.970E-03
104	608.925E+06	0.	905.973E-03
105	319.917E+06	0.	869.161E-03
106	108.557E+06	0.	843.258E-03
107	380.168E+06	0.	805.140E-03
108	403.473E+06	0.	781.328E-03
109	530.895E+06	0.	755.832E-03
110	305.100E+06	0.	746.397E-03
111	172.971E+06	0.	720.303E-03
112	298.548E+06	0.	712.450E-03
113	178.280E+06	0.	1.48648
114	2.82185E+09	0.	709.404E-03
115	1.85782E+09	0.	572.623E-03
116	3.47907E+09	0.	681.325E-03
117	2.56230E+09	0.	681.279E-03
118	1.14702E+09	0.	604.765E-03
119	2.74259E+09	0.	852.761E-03
120	1.50962E+09	0.	1.18011
121	1.29805E+09	0.	1.24200
122	3.04222E+09	0.	1.24242
123	2.13768E+09	0.	1.21685
124	1.07609E+09	0.	1.19669
125	3.57259E+09	0.	1.20308
126	2.65245E+09	0.	1.24562
127	3.48727E+09	0.	1.24857
128	4.66482E+09	0.	1.22738
129	2.62943E+09	0.	1.25205
130	2.46170E+09	0.	1.27158
131	2.71131E+09	0.	1.25804
132	1.56387E+09	0.	1.27390
133	3.63321E+09	0.	1.15739
134	4.99771E+09	0.	1.14924
135	6.70143E+09	0.	1.20826
136	5.25859E+09	0.	871.632E-03
137	3.85637E+09	0.	1.13028
138	50.6706E+09	0.	1.81004
139	495.354E+06	0.	1.39024
140	7.11959E+09	0.	1.15690
141	5.95259E+09	0.	1.00425
142	3.28750E+09	0.	705.894E-03
143	8.64743E+09	0.	744.239E-03
144	10.2115E+09	0.	738.016E-03

145	7.85562E+09	0.	860.596E-03
146	2.07535E+09	0.	1.01737
147	14.3013E+09	0.	679.897E-03
148	11.5315E+09	0.	1.04247
149	12.8813E+09	0.	848.484E-03
150	10.5796E+09	0.	880.716E-03
151	12.5454E+09	0.	926.419E-03
152	11.3172E+09	0.	981.104E-03
153	16.5617E+09	0.	955.175E-03
154	14.3646E+09	0.	931.010E-03
155	14.2054E+09	0.	1.04434
156	16.2354E+09	0.	884.066E-03
157	10.7567E+09	0.	857.338E-03
158	7.93602E+09	0.	827.968E-03
159	9.52904E+09	0.	960.983E-03
160	10.0853E+09	0.	889.188E-03
161	8.89414E+09	0.	772.073E-03
162	9.49394E+09	0.	638.872E-03
163	12.1541E+09	0.	735.110E-03
164	4.09822E+09	0.	967.393E-03
165	252.061E+06	0.	720.347E-03
166	249.604E+06	0.	733.700E-03
167	259.106E+06	0.	771.648E-03
168	428.082E+06	0.	811.841E-03
169	328.124E+06	0.	885.014E-03
170	125.398E+06	0.	900.840E-03
171	123.890E+06	0.	969.603E-03
172	309.375E+06	0.	1.00484
173	500.615E+06	0.	1.03672
174	656.769E+06	0.	1.04955
175	559.834E+06	0.	1.06171
176	952.001E+06	0.	1.05527
177	478.888E+06	0.	1.09613
178	801.066E+06	0.	1.08576
179	619.881E+06	0.	1.10863
180	838.412E+06	0.	1.14056
181	601.645E+06	0.	1.14665
182	289.786E+06	0.	1.04203
183	265.652E+06	0.	1.00553
184	532.665E+06	0.	949.471E-03
185	607.460E+06	0.	898.782E-03
186	502.963E+06	0.	936.890E-03
187	657.966E+06	0.	901.788E-03
188	703.972E+06	0.	886.430E-03
189	162.332E+06	0.	838.387E-03
190	403.531E+06	0.	855.353E-03
191	248.870E+06	0.	808.044E-03
192	580.182E+06	0.	784.008E-03
193	464.997E+06	0.	757.618E-03
194	333.125E+06	0.	757.095E-03
195	392.581E+06	0.	746.045E-03
196	578.763E+06	0.	717.249E-03
197	694.200E+06	0.	720.815E-03
198	472.769E+06	0.	717.751E-03
199	89.4586E+06	0.	1.43923
200	4.34200E+09	0.	697.700E-03
201	5.85498E+09	0.	874.846E-03

202	9.36981E+09	0.	992.776E-03
203	14.4385E+09	0.	993.860E-03
204	9.24077E+09	0.	1.07401
205	4.78440E+09	0.	1.12677
206	4.54297E+09	0.	1.09540
207	4.67768E+09	0.	1.18397
208	5.38574E+09	0.	1.17482
209	3.82041E+09	0.	1.17355
210	1.86610E+09	0.	1.00720
211	5.14781E+09	0.	885.528E-03
212	2.76607E+09	0.	972.228E-03
213	3.42677E+09	0.	996.887E-03
214	2.40333E+09	0.	1.00312
215	8.48646E+09	0.	664.418E-03
216	1.55279E+09	0.	710.554E-03
217	7.69130E+09	0.	777.173E-03
218	12.6294E+09	0.	898.887E-03
219	6.15108E+09	0.	839.206E-03
220	9.20495E+09	0.	797.050E-03
221	5.47432E+09	0.	873.084E-03
222	3.67783E+09	0.	866.454E-03
223	5.21940E+09	0.	906.090E-03
224	6.27385E+09	0.	626.395E-03
225	9.54067E+09	0.	731.776E-03
226	3.93830E+09	0.	851.370E-03
227	7.08012E+09	0.	693.313E-03
228	4.17690E+09	0.	895.205E-03
229	4.93742E+09	0.	1.07079
230	3.16196E+09	0.	988.292E-03
231	4.68264E+09	0.	948.800E-03
232	6.91400E+09	0.	795.369E-03
233	5.31987E+09	0.	648.975E-03
234	5.01716E+09	0.	771.326E-03
235	6.38759E+09	0.	917.047E-03
236	3.68565E+09	0.	902.874E-03
237	1.39855E+09	0.	889.490E-03
238	3.98558E+09	0.	955.055E-03
239	10.4272E+09	0.	903.862E-03
240	9.79986E+09	0.	861.722E-03
241	4.08967E+09	0.	666.315E-03
242	4.20508E+09	0.	671.619E-03
243	3.65869E+09	0.	728.888E-03
244	2.89401E+09	0.	815.258E-03
245	3.32078E+09	0.	816.094E-03
246	3.47466E+09	0.	704.591E-03
247	2.08412E+09	0.	943.721E-03
248	5.77130E+09	0.	984.298E-03

Spacial displacement, acceleration magnitudes and reaction forces for Inverted u-shaped RC shaer wall with a central load orientation

```
******************************************************************************
*********
Field Output Report, written Tue Nov 01 11:53:36 2016

Source 1
---------

   ODB: C:/Users/him/ABAQUS Temp file/orie-1.odb
   Step: blast load
   Frame: Increment       319: Step Time =   1.0000E-03

Loc 1 : Nodal values from source 1

Output sorted by column "Node Label".

Field Output reported at nodes for part: horizontal bar 1-1
   Computation algorithm: EXTRAPOLATE_COMPUTE_AVERAGE
   Averaged at nodes
   Averaging regions: ODB_REGIONS

            Node    RF.Magnitude     U.Magnitude    PE.Max. Prin
           Label          @Loc 1          @Loc 1          @Loc 1
-----------------------------------------------------------------
               1              0.         883.539     185.080E-03
               2              0.         581.377     760.952E-03
               3              0.         845.836     154.312E-03
               4              0.         611.495     800.135E-03
               5              0.         844.288     156.812E-03
               6              0.         612.615     804.102E-03
               7              0.         845.247     155.749E-03
               8              0.         612.699     803.885E-03
               9              0.         880.476     180.365E-03
              10              0.         637.681     802.712E-03
              11              0.     1.13646E+03     324.055E-03
              12              0.         918.131         1.01297
              13              0.         845.377     158.159E-03
              14              0.         614.048     803.086E-03
              15              0.         845.191     156.339E-03
              16              0.         612.810     804.771E-03
              17              0.         844.348     153.420E-03
              18              0.         612.114     802.802E-03
              19              0.         851.113     162.476E-03
              20              0.         615.523     803.653E-03
              21              0.         281.558     121.589E-03
              22              0.         139.047     161.880E-03
              23              0.         720.911     92.5398E-03
              24              0.         701.070     11.7790E-03
              25              0.         712.087     205.544E-03
              26              0.         738.935     574.241E-03
              27              0.         773.507     77.1558E-03
              28              0.         754.172              0.
              29              0.         757.595     194.722E-03
              30              0.         754.454     594.789E-03
```

31	0.	771.430	78.4059E-03
32	0.	750.995	0.
33	0.	756.053	194.367E-03
34	0.	756.338	596.418E-03
35	0.	772.330	77.8746E-03
36	0.	752.554	0.
37	0.	757.275	193.908E-03
38	0.	756.919	595.850E-03
39	0.	796.356	90.1824E-03
40	0.	774.226	4.64081E-03
41	0.	780.393	213.860E-03
42	0.	779.322	610.575E-03
43	0.	875.414	162.027E-03
44	0.	843.828	98.7298E-06
45	0.	867.912	284.098E-03
46	0.	1.02370E+03	790.487E-03
47	0.	772.102	79.0797E-03
48	0.	752.770	361.603E-06
49	0.	758.178	193.970E-03
50	0.	757.888	595.151E-03
51	0.	772.572	78.1695E-03
52	0.	752.280	0.
53	0.	757.029	193.920E-03
54	0.	756.919	596.306E-03
55	0.	771.433	76.7099E-03
56	0.	751.499	0.
57	0.	755.398	194.811E-03
58	0.	755.226	596.212E-03
59	0.	773.683	81.2382E-03
60	0.	754.625	5.42965E-03
61	0.	759.553	198.502E-03
62	0.	760.884	594.899E-03
63	0.	201.879	60.7947E-03
64	0.	193.759	6.29939E-03
65	0.	199.212	57.4540E-03
66	0.	173.526	132.095E-03
Minimum	0.	139.047	0.
At Node	66	22	56
Maximum	0.	1.13646E+03	1.01297
At Node	66	11	12
Total	0.	47.3292E+03	19.6543

Field Output reported at nodes for part: horizontal bar 1-1-1
Computation algorithm: EXTRAPOLATE_COMPUTE_AVERAGE
Averaged at nodes
Averaging regions: ODB_REGIONS

Node Label	RF.Magnitude @Loc 1	U.Magnitude @Loc 1	PE.Max. Prin @Loc 1
1	0.	948.572	246.434E-03
2	0.	631.073	1.02970

3	0.	888.203	143.826E-03
4	0.	648.819	1.05788
5	0.	886.399	147.285E-03
6	0.	649.387	1.06131
7	0.	886.914	146.688E-03
8	0.	649.603	1.06059
9	0.	922.148	172.311E-03
10	0.	668.878	1.06063
11	0.	1.24961E+03	424.745E-03
12	0.	994.911	1.31656
13	0.	885.181	145.840E-03
14	0.	650.650	1.05795
15	0.	887.116	146.867E-03
16	0.	649.486	1.06209
17	0.	886.550	145.467E-03
18	0.	649.230	1.06003
19	0.	898.485	151.061E-03
20	0.	653.529	1.06009
21	0.	230.195	81.7409E-03
22	0.	134.439	277.569E-03
23	0.	748.461	123.217E-03
24	0.	734.941	13.4980E-03
25	0.	751.051	189.146E-03
26	0.	811.400	690.498E-03
27	0.	781.333	79.3541E-03
28	0.	759.161	10.5645E-03
29	0.	766.227	162.886E-03
30	0.	805.031	688.704E-03
31	0.	778.938	81.9343E-03
32	0.	755.733	10.7209E-03
33	0.	763.316	161.346E-03
34	0.	807.341	689.572E-03
35	0.	779.740	82.3571E-03
36	0.	757.198	11.5860E-03
37	0.	764.910	161.680E-03
38	0.	808.076	689.403E-03
39	0.	808.954	100.939E-03
40	0.	783.031	27.0152E-03
41	0.	792.376	182.596E-03
42	0.	825.040	700.679E-03
43	0.	919.051	212.373E-03
44	0.	886.027	13.2003E-03
45	0.	913.893	297.879E-03
46	0.	1.12936E+03	942.959E-03
47	0.	780.105	84.9579E-03
48	0.	757.704	17.8690E-03
49	0.	766.565	164.863E-03
50	0.	807.355	688.008E-03
51	0.	779.962	81.7273E-03
52	0.	756.942	10.4253E-03
53	0.	764.285	160.580E-03
54	0.	807.902	689.494E-03
55	0.	779.134	80.5358E-03
56	0.	756.333	10.4103E-03
57	0.	762.817	162.529E-03
58	0.	805.929	689.936E-03
59	0.	781.566	81.9404E-03

60	0.	761.093	15.8594E-03
61	0.	772.328	170.698E-03
62	0.	815.378	691.296E-03
63	0.	183.885	40.8704E-03
64	0.	184.370	2.57586E-03
65	0.	183.982	34.0400E-03
66	0.	157.636	170.249E-03
Minimum	0.	134.439	2.57586E-03
At Node	66	22	64
Maximum	0.	1.24961E+03	1.31656
At Node	66	11	12
Total	0.	49.1452E+03	23.4296

```
Field Output reported at nodes for part: horizontal bar 2-1
   Computation algorithm: EXTRAPOLATE_COMPUTE_AVERAGE
   Averaged at nodes
   Averaging regions: ODB_REGIONS
```

Node Label	RF.Magnitude @Loc 1	U.Magnitude @Loc 1	PE.Max. Prin @Loc 1
1	0.	671.080	1.07127
2	0.	668.180	1.06005
3	0.	652.859	1.07000
4	0.	649.024	1.06041
5	0.	652.692	1.07035
6	0.	649.016	1.06079
7	0.	651.358	1.06722
8	0.	647.741	1.05752
9	0.	635.422	1.03925
10	0.	632.212	1.03448
11	0.	130.985	276.717E-03
12	0.	134.460	277.407E-03
13	0.	656.261	1.06957
14	0.	653.046	1.05907
15	0.	651.852	1.06893
16	0.	648.393	1.05997
17	0.	652.666	1.07097
18	0.	648.954	1.06117
19	0.	653.607	1.06723
20	0.	649.787	1.05829
21	0.	997.781	1.33137
22	0.	993.868	1.31030
23	0.	822.521	695.140E-03
24	0.	794.342	193.311E-03
25	0.	794.572	207.453E-03
26	0.	823.660	703.672E-03
27	0.	805.382	682.215E-03
28	0.	767.831	169.413E-03
29	0.	768.173	183.181E-03
30	0.	807.831	691.189E-03
31	0.	804.422	682.833E-03

32	0.	766.446	168.130E-03
33	0.	766.887	181.745E-03
34	0.	807.015	691.666E-03
35	0.	802.348	680.696E-03
36	0.	768.412	169.736E-03
37	0.	768.754	183.599E-03
38	0.	804.742	689.707E-03
39	0.	807.348	680.713E-03
40	0.	751.750	195.327E-03
41	0.	752.200	208.057E-03
42	0.	810.485	691.058E-03
43	0.	160.916	167.709E-03
44	0.	184.833	36.2626E-03
45	0.	184.866	38.2730E-03
46	0.	157.935	170.064E-03
47	0.	814.042	685.631E-03
48	0.	774.980	183.400E-03
49	0.	775.449	197.587E-03
50	0.	816.873	694.565E-03
51	0.	803.086	682.351E-03
52	0.	765.622	167.503E-03
53	0.	765.989	180.726E-03
54	0.	805.514	691.093E-03
55	0.	805.063	682.756E-03
56	0.	767.313	168.236E-03
57	0.	767.735	182.238E-03
58	0.	807.718	691.861E-03
59	0.	805.013	681.789E-03
60	0.	769.315	173.949E-03
61	0.	769.544	187.129E-03
62	0.	807.005	690.497E-03
63	0.	1.12290E+03	932.367E-03
64	0.	915.981	303.375E-03
65	0.	917.999	342.732E-03
66	0.	1.14571E+03	961.186E-03
Minimum	0.	130.985	36.2626E-03
At Node	66	11	44
Maximum	0.	1.14571E+03	1.33137
At Node	66	66	21
Total	0.	47.1878E+03	40.9445

Special displacement, acceleration, reaction forces and plastic maximum strain for some nodes

```
********************************************************************************
Field Output Report, written Tue Nov 01 12:02:41 2016

Source 1
---------

   ODB: C:/Users/him/ABAQUS Temp file/Jo-80.odb
   Step: blast
   Frame: Increment      2554: Step Time =   3.0000E-04

Loc 1 : Nodal values from source 1

Output sorted by column "Node Label".

Field Output reported at nodes for part: CONCRETE-1
   Computation algorithm: EXTRAPOLATE_COMPUTE_AVERAGE
   Averaged at nodes
   Averaging regions: ODB_REGIONS

            Node     A.Magnitude    RF.Magnitude     U.Magnitude
PE.Max. Prin
           Label          @Loc 1          @Loc 1          @Loc 1
@Loc 1
--------------------------------------------------------------------------------
               1              0.     199.174E+06              0.
624.537E-03
               2              0.     1.35124E+09              0.
822.619E-03
               3              0.     568.906E+06              0.
1.10053
               4              0.     472.855E+06              0.
1.20648
               5              0.     383.843E+06              0.
1.24068
               6              0.     333.405E+06              0.
1.24969
               7              0.     312.108E+06              0.
1.24934
               8              0.     319.472E+06              0.
1.23954
               9              0.     584.081E+06              0.
1.20460
              10              0.     470.255E+06              0.
1.10411
              11              0.     1.24663E+09              0.
830.848E-03
              12              0.     381.238E+06              0.
631.629E-03
              13              0.     128.887E+06              0.
624.537E-03
```

14	0.	163.297E+06	0.	822.619E-03
15	0.	1.54039E+09	0.	1.10053
16	0.	1.04073E+09	0.	1.20648
17	0.	438.633E+06	0.	1.24068
18	0.	404.723E+06	0.	1.24969
19	0.	376.652E+06	0.	1.24934
20	0.	510.135E+06	0.	1.23954
21	0.	933.025E+06	0.	1.20460
22	0.	1.53516E+09	0.	1.10411
23	0.	253.764E+06	0.	830.848E-03
24	0.	99.5582E+06	0.	631.629E-03
25	0.	872.797E+06	0.	824.534E-03
26	821.644E+09	0.	139.758	835.428E-03
27	413.022E+09	0.	205.572	895.549E-03
28	222.951E+09	0.	242.425	976.873E-03
29	349.069E+09	0.	252.419	1.02620
30	90.0881E+09	0.	258.413	1.04605
31	171.127E+09	0.	259.387	1.04386
32	185.711E+09	0.	254.448	1.02244
33	159.469E+09	0.	239.606	972.446E-03
34	1.20777E+12	0.	205.976	895.259E-03
35	1.85586E+12	0.	141.294	842.578E-03
36	0.	982.277E+06	0.	833.720E-03
37	0.	303.017E+06	0.	824.534E-03
38	503.929E+09	0.	123.080	835.428E-03
39	621.734E+09	0.	183.687	895.549E-03
40	35.7599E+09	0.	209.489	976.873E-03
41	67.8498E+09	0.	218.300	1.02620

42	111.411E+09	0.	221.426	1.04605
43	32.8595E+09	0.	221.101	1.04386
44	133.874E+09	0.	219.401	1.02244
45	180.903E+09	0.	207.156	972.446E-03
46	1.76359E+12	0.	184.628	895.259E-03
47	1.31238E+12	0.	123.986	842.578E-03
48	0.	313.936E+06	0.	833.720E-03
49	0.	577.509E+06	0.	1.09128
50	994.061E+09	0.	204.294	903.451E-03
51	269.685E+09	0.	278.438	699.878E-03
52	80.2488E+09	0.	343.913	738.293E-03
53	130.123E+09	0.	374.776	821.453E-03
54	151.393E+09	0.	384.278	858.162E-03
55	25.5916E+09	0.	385.176	852.394E-03
56	26.5004E+09	0.	373.257	812.053E-03
57	63.3123E+09	0.	341.963	754.199E-03
58	1.52461E+12	0.	280.022	708.761E-03
59	1.90128E+12	0.	210.635	901.834E-03
60	0.	242.145E+06	0.	1.10936
61	0.	873.114E+06	0.	1.09128
62	180.688E+09	0.	182.353	903.451E-03
63	452.532E+09	0.	282.198	699.878E-03
64	125.484E+09	0.	347.407	738.293E-03
65	53.9747E+09	0.	374.732	821.453E-03
66	98.7279E+09	0.	383.076	858.162E-03
67	83.6894E+09	0.	384.012	852.394E-03
68	46.8028E+09	0.	374.223	812.053E-03
69	75.7852E+09	0.	346.435	754.199E-03

70	763.016E+09	0.	283.076	708.761E-03
71	1.95185E+12	0.	186.362	901.834E-03
72	0.	1.44384E+09	0.	1.10936
73	0.	1.00312E+09	0.	1.19125
74	332.569E+09	0.	229.425	1.01524
75	956.497E+09	0.	340.830	801.823E-03
76	94.0265E+09	0.	438.206	790.762E-03
77	76.9405E+09	0.	491.912	851.464E-03
78	68.1133E+09	0.	517.632	902.974E-03
79	38.1725E+09	0.	516.626	904.244E-03
80	43.1510E+09	0.	489.441	852.971E-03
81	36.9960E+09	0.	439.396	827.406E-03
82	330.268E+09	0.	336.640	814.230E-03
83	1.13310E+12	0.	238.583	1.00217
84	0.	1.22435E+09	0.	1.21313
85	0.	595.273E+06	0.	1.19125
86	998.141E+09	0.	196.939	1.01524
87	531.890E+09	0.	353.509	801.823E-03
88	58.3941E+09	0.	455.479	790.762E-03
89	16.1795E+09	0.	509.193	851.464E-03
90	6.43213E+09	0.	528.862	902.974E-03
91	22.1526E+09	0.	527.478	904.244E-03
92	43.3229E+09	0.	503.732	852.971E-03
93	40.3271E+09	0.	453.544	827.406E-03
94	86.9989E+09	0.	336.845	814.230E-03
95	391.800E+09	0.	209.274	1.00217
96	0.	433.466E+06	0.	1.21313
97	0.	537.305E+06	0.	1.24202

98	281.837E+09	0.	249.964	1.10863
99	156.696E+09	0.	388.237	966.172E-03
100	31.7830E+09	0.	532.579	903.323E-03
101	108.712E+09	0.	619.972	855.045E-03
102	44.9041E+09	0.	673.844	851.071E-03
103	87.8319E+09	0.	678.421	852.857E-03
104	31.8220E+09	0.	621.200	855.919E-03
105	19.2251E+09	0.	540.483	928.937E-03
106	60.8119E+09	0.	386.288	967.463E-03
107	613.727E+09	0.	259.907	1.09075
108	0.	307.315E+06	0.	1.25672
109	0.	848.831E+06	0.	1.24202
110	266.152E+09	0.	227.975	1.10863
111	53.3308E+09	0.	406.423	966.172E-03
112	27.1229E+09	0.	558.065	903.323E-03
113	88.2476E+09	0.	647.618	855.045E-03
114	23.3709E+09	0.	699.336	851.071E-03
115	96.1981E+09	0.	702.620	852.857E-03
116	26.9471E+09	0.	645.726	855.919E-03
117	47.9008E+09	0.	562.399	928.937E-03
118	186.821E+09	0.	391.786	967.463E-03
119	605.936E+09	0.	227.887	1.09075
120	0.	1.25978E+09	0.	1.25672
121	0.	169.619E+06	0.	1.27384
122	288.565E+09	0.	269.443	1.16958
123	542.181E+09	0.	426.011	1.08450
124	61.4823E+09	0.	619.806	960.136E-03
125	50.9465E+09	0.	731.397	736.049E-03

126	48.6651E+09	0.	793.609	595.233E-03
127	37.1095E+09	0.	789.902	588.147E-03
128	72.3702E+09	0.	733.077	714.429E-03
129	87.1723E+09	0.	626.565	962.975E-03
130	4.99953E+09	0.	419.491	1.08360
131	214.876E+09	0.	266.982	1.15499
132	0.	424.598E+06	0.	1.28121
133	0.	913.288E+06	0.	1.27384
134	262.385E+09	0.	239.875	1.16958
135	466.513E+09	0.	440.749	1.08450
136	21.1040E+09	0.	648.560	960.136E-03
137	17.1417E+09	0.	763.613	736.049E-03
138	39.7491E+09	0.	827.265	595.233E-03
139	49.9699E+09	0.	824.105	588.147E-03
140	88.0319E+09	0.	763.958	714.429E-03
141	20.6651E+09	0.	647.928	962.975E-03
142	46.7952E+09	0.	424.270	1.08360
143	148.340E+09	0.	229.615	1.15499
144	0.	478.332E+06	0.	1.28121
145	0.	485.659E+06	0.	1.29348
146	220.980E+09	0.	274.751	1.20750
147	49.5555E+09	0.	446.613	1.15938
148	71.8554E+09	0.	672.651	958.507E-03
149	68.4081E+09	0.	780.120	576.425E-03

```
********************************************************************************
Field Output Report, written Sun Nov 13 05:49:18 2016

Source 1
---------

   ODB: C:/Users/him/ABAQUS Temp file/Jolas-5.odb
   Step: blast 11
   Frame: Increment     31867: Step Time =   4.5000E-04

Loc 1 : Integration point values from source 1

Output sorted by column "Element Label".

Field Output reported at integration points for part: CONCRET-1

         Element             Int      S.Pressure
          Label               Pt          @Loc 1
-------------------------------------------------
               1               1     3.04205E+03
               2               1         459.295
               3               1         89.1835
               4               1         53.2393
               5               1        -21.6037
               6               1         6.57822
               7               1         224.102
               8               1        -20.2484
               9               1        -19.2779
              10               1        -16.3575
              11               1        -18.8611
              12               1        -18.2885
              13               1         51.2235
              14               1         9.42724
              15               1         119.284
              16               1         55.2468
              17               1        -10.4585
              18               1         53.7736
              19               1         58.4680
              20               1         55.2970
              21               1         221.660
              22               1         236.084
              23               1         413.367
              24               1         399.634
              25               1         196.138
              26               1         200.334
              27               1         7.98053
              28               1    -416.681E-03
              29               1         54.2719
              30               1        -11.0714
              31               1        -12.1792
              32               1         10.7192
              33               1         16.9641
              34               1         17.2723
              35               1        -6.32135
              36               1        -19.0779
              37               1         17.2410
```

38	1	5.88564
39	1	-10.6760
40	1	-14.7818
41	1	5.49912
42	1	-15.3669
43	1	-14.6153
44	1	54.2261
45	1	-10.7876
46	1	-1.14541
47	1	27.3354
48	1	-9.23389
49	1	-16.2522
50	1	-19.0608
51	1	-15.5254
52	1	26.8051
53	1	41.2182
54	1	-16.9367
55	1	-17.6330
56	1	-19.2056
57	1	-16.7989
58	1	-15.5713
59	1	-17.9600
60	1	4.55052
61	1	11.5079
62	1	11.1797
63	1	-19.7810
64	1	-15.8582
65	1	-19.7561
66	1	-15.0555
67	1	2.04919
68	1	-19.5900
69	1	-4.91385
70	1	-17.6746
71	1	-20.7332
72	1	2.14746
73	1	-11.2667
74	1	-20.0197
75	1	-18.0073
76	1	20.5257
77	1	8.11375
78	1	7.15444
79	1	-3.00765
80	1	-18.1870
81	1	-16.0825
82	1	-12.5043
83	1	-14.2255
84	1	-13.9563
85	1	-15.7175
86	1	8.01906
87	1	1.41732
88	1	13.0190
89	1	-19.2080
90	1	-20.5954
91	1	-17.9742
92	1	-19.9576
93	1	-19.8122
94	1	-12.2295

95	1	-5.42309
96	1	-14.0453
97	1	-18.1488
98	1	17.6428
99	1	-12.6266
100	1	-17.1962
101	1	-15.5271
102	1	18.6549
103	1	12.1984
104	1	-18.6407
105	1	-17.8141
106	1	-16.5082
107	1	-17.2160
108	1	-16.8989
109	1	3.59927
110	1	31.2034
111	1	-204.717E-03
112	1	5.82944
113	1	-20.1593
114	1	-16.3522
115	1	-18.9180
116	1	-18.3084
117	1	2.93883
118	1	25.5962
119	1	-12.7322
120	1	-7.68079
121	1	-9.13529
122	1	1.79186
123	1	-5.03002
124	1	11.9487
125	1	2.01686
126	1	-17.3424
127	1	-15.7362
128	1	-18.0582
129	1	-18.3287
130	1	-16.3101
131	1	-3.56789
132	1	8.54589
133	1	31.2883
134	1	-5.45355
135	1	-4.60542
136	1	-18.5257
137	1	-20.6900
138	1	-20.5762
139	1	6.08877
140	1	44.3570
141	1	-17.7789
142	1	-19.3256